

Supporting Information

Rapid Access to (Cycloalkyl)tellurophene Oligomer Mixtures and the First Poly(3-aryltellurophene)

Bruno T. Luppi, Robert McDonald, Michael J. Ferguson, Lingzi Sang* and Eric Rivard*

Department of Chemistry, University of Alberta, 11227 Saskatchewan Drive, Edmonton, Alberta, Canada T6G 2G2

Table of Contents:

| | |
|--|-----|
| 1. <u>General Information, Materials and Instrumentation</u> | S3 |
| 2. <u>Experimental Procedures</u> | S4 |
| 3. <u>DFT Computations</u> | S12 |
| Computational details | S12 |
| Fig. S1. Structure optimization of heptamers of Oligo-Te6 and Oligo-Te5 . | S13 |
| Fig. S2. Energy change of oligomers upon change of the torsional angle between the chalcogenophenes | S13 |
| Table S1. Computed excited states of trimers of Oligo-Te5 (I-[Te5]3-I) and Oligo-Te6 (I-[Te6]3-I) by TD-DFT. | S14 |
| Fig. S3. Computed UV-Vis absorptivity for trimers of Oligo-Te5 (I-[Te5]3-I) and Oligo-Te6 (I-[Te6]3-I) and the three main oscillator strengths (bars below the curves) associated with the absorptions. | S15 |
| 4. <u>X-Ray Crystallography</u> | S16 |
| Fig. S4. Molecular structure of 1,3-diiodo-4,5,6,7-tetrahydro-benzo[c]tellurophene (I-Te-6-I). | S16 |
| Table S2. Crystallographic experimental details for 1,3-diiodo-4,5,6,7-tetrahydro-benzo[c]-tellurophene (I-Te-6-I). | S16 |
| Fig. S5. Molecular structure of 1,3-diiodo-4,5,6,7-tetrahydro-cyclopenta[c]-tellurophene (I-Te-5-I). | S18 |
| Table S3. Crystallographic experimental details for 1,3-diiodo-4,5,6,7-tetrahydro-cyclopenta[c]-tellurophene (I-Te-5-I). | S18 |
| Fig. S6. Molecular structure of 3-(4-isopropylphenyl)-tellurophene (Te-cumenyl). | S20 |
| Table S4. Crystallographic experimental details for 3-(4-isopropylphenyl)-tellurophene (Te-cumenyl). | S20 |
| 5. <u>NMR Spectroscopy</u> | S22 |
| Fig. S7. ¹ H NMR spectrum (500 MHz) of 1,3-diiodo-4,5,6,7-tetrahydro-benzo[c]tellurophene (I-Te-6-I) in CDCl ₃ . | S22 |
| Fig. S8. ¹³ C{ ¹ H} NMR spectrum (126 MHz) of 1,3-diiodo-4,5,6,7-tetrahydro-benzo[c]tellurophene (I-Te-6-I) in CDCl ₃ . | S22 |
| Fig. S9. ¹ H NMR spectrum (500 MHz) of 1,3-diiodo-4,5,6,7-tetrahydro-cyclopenta[c]-tellurophene (I-Te-5-I) in CDCl ₃ ; BHT = butylated hydroxytoluene. | S23 |
| Fig. S10. ¹³ C{ ¹ H} NMR spectrum (126 MHz) of 1,3-diiodo-4,5,6,7-tetrahydro-cyclopenta[c]-tellurophene (I-Te-5-I) in CDCl ₃ . | S23 |
| Fig. S11. ¹ H NMR spectrum (500 MHz) of Oligo-Te5 in CDCl ₃ . | S24 |
| Fig. S12. ¹ H NMR spectrum (400 MHz) of Oligo-Te6 in CDCl ₃ . | S24 |
| Fig. S13. ¹ H NMR spectrum (400 MHz) of 3-(4-isopropylphenyl)-tellurophene (Te-cumenyl) in CDCl ₃ . | S25 |
| Fig. S14. ¹³ C{ ¹ H} NMR spectrum (126 MHz) of 3-(4-isopropylphenyl)-tellurophene (Te-cumenyl) in CDCl ₃ ; BHT = butylated hydroxytoluene. | S25 |

| | |
|---|-----|
| Fig. S15. ^1H NMR spectrum (700 MHz) of 2-iodo-3-(4-isopropylphenyl)-tellurophene (I-Te-cumenyl) in CDCl_3 . | S26 |
| Fig. S16. $^{13}\text{C}\{^1\text{H}\}$ NMR spectrum (176 MHz) of 2-iodo-3-(4-isopropylphenyl)-tellurophene (I-Te-cumenyl) in CDCl_3 . | S26 |
| Fig S17. ^1H NMR spectrum (500 MHz) of 2,5-diiodo-3-(4-isopropylphenyl)-tellurophene (I-Te-cumenyl-I) in CDCl_3 . | S27 |
| Fig. S18. $^{13}\text{C}\{^1\text{H}\}$ NMR spectrum (126 MHz) of 2,5-diiodo-3-(4-isopropylphenyl)-tellurophene (I-Te-cumenyl-I) in CDCl_3 . | S27 |
| Fig. S19. ^1H NMR spectrum (500 MHz) of 3-(4-isopropylphenyl)-thiophene (S-cumenyl) in CDCl_3 . | S28 |
| Fig. S20. $^{13}\text{C}\{^1\text{H}\}$ NMR spectrum (126 MHz) of 3-(4-isopropylphenyl)-thiophene (S-cumenyl) in CDCl_3 . | S28 |
| Fig. S21. ^1H NMR spectrum (400 MHz) of 2,5-diiodo-3-(4-isopropylphenyl)-thiophene (I-S-cumenyl-I) in CDCl_3 . | S29 |
| Fig. S22. $^{13}\text{C}\{^1\text{H}\}$ NMR spectrum (101 MHz) of 2,5-diiodo-3-(4-isopropylphenyl)-thiophene (I-S-cumenyl-I) in CDCl_3 . | S29 |
| Fig. S23. ^1H NMR spectrum (400 MHz) of poly(3-(4-isopropylphenyl)-thiophene) (PolyS-cumenyl) in CDCl_3 . | S30 |
| Fig. S24. ^1H NMR spectrum (500 MHz) of poly(3-(4-isopropylphenyl)-tellurophene) (PolyTe-cumenyl) in CDCl_3 . | S30 |
| Fig. S25. ^1H NMR spectrum study of GRIM activation step for I-S-cumenyl-I (a) and I-Te-cumenyl-I (b) at different temperatures after quenching the reaction with dilute HCl. | S31 |
| Fig. S26. ^1H NMR of the isopropyl region of polymers with low regioselectivity obtained during GRIM polymerization trials with $\text{Ni}(\text{dppe})\text{Cl}_2$ (1 mol%). | S32 |
| | |
| 6. <u>UV-Vis Spectroscopy</u> | S33 |
| Fig. S27. UV-Vis spectra of I-Te-5-I and I-Te-6-I in THF and the respective oligomer mixtures Oligo-Te5 and Oligo-Te6 in CHCl_3 . | S33 |
| Fig. S28. UV-Vis spectra of Oligo-Te6 and Oligo-Te5 (as drop-cast films from CHCl_3) before and after annealing at 70 °C. | S33 |
| Fig. S29. UV-Vis spectra of I-S-cumenyl-I and I-Te-cumenyl-I in THF. | S34 |
| Fig. S30. UV-Vis spectra of PolyS-cumenyl (a) and PolyTe-cumenyl (b) in THF at different concentrations. | S34 |
| Fig. S31. Determination of onset of absorption for films of PolyTe-cumenyl . | S35 |
| | |
| 7. <u>MALDI Mass Spectrometry</u> | S36 |
| Fig. S32. MALDI-MS spectrum of Oligo-Te6 . | S36 |
| Fig. S33. MALDI-MS spectrum of Oligo-Te5 . | S36 |
| Fig. S34. MALDI-MS of a self-oligomerized sample of I-Te-6-I . | S37 |
| Fig. S35. MALDI-MS of a self-oligomerized sample of I-Te-5-I . | S37 |
| Fig. S36. MALDI-MS spectrum of PolyS-cumenyl . | S38 |
| Fig. S37. MALDI-MS spectrum of PolyTe-cumenyl . | S38 |
| Fig. S38. MALDI-MS of PolyS-cumenyl and PolyTe-cumenyl prepared with $\text{Ni}(\text{dppe})\text{Cl}_2$. | S39 |
| | |
| 8. <u>Gel Permeation Chromatography</u> | S40 |
| Fig. S39. GPC elution profile for PolyS-cumenyl . | S40 |
| Fig. S40. GPC elution profile for PolyTe-cumenyl . | S40 |
| | |
| 9. <u>TGA and DSC Data</u> | S41 |
| Fig. S41. TGA of I-Te-6-I and I-Te-5-I (left) and the black precipitate formed upon degradation of I-Te-5-I (right) obtained at 10 °C/min. | S41 |
| Fig. S42. TGA of Oligo-Te6 (left) and Oligo-Te5 (right) obtained at 10 °C/min. | S41 |
| Fig. S43. TGA of I-S-cumenyl-I (left) and I-Te-cumenyl-I (right) obtained at 10 °C/min. | S41 |
| Fig. S44. TGA of PolyS-cumenyl (left) and PolyTe-cumenyl (right) obtained at 10 °C/min. | S42 |
| Fig. S45. DSC of PolyS-cumenyl (left) and PolyTe-cumenyl (right) obtained at 20 °C/min. | S42 |

| | |
|---|-----|
| 10. <u>Cyclic Voltammetry</u> | S43 |
| Fig. S46. Cyclic voltammograms of PolyTe-cumenyl and PolyS-cumenyl films on ITO. | S43 |
| Fig. S47. Cyclic voltammogram of PolyTe-cumenyl over different cycles. | S43 |
| 11. <u>Powder XRD</u> | S44 |
| Fig. S48. Powder XRD of PolyTe-cumenyl and PolyS-cumenyl before and after solvent vapor annealing. | S44 |
| 12. <u>References</u> | S44 |

1. General Information, Materials and Instrumentation

Unless specified, all reactions were performed under inert atmosphere of N₂ by using Schlenk techniques or a glovebox (MBraun) with dry and degassed solvents from a Grubbs-type solvent system (manufactured by Innovative Technology Inc.) Microwave reactions were performed on a Biotage Initiator reactor. DMF was dried over 4 Å molecular sieves and degassed via three freeze-pump-thaw cycles. 4-Isopropylphenylboronic acid,¹ PinBC≡C(CH₂)₄C≡CBPin² and PinBC≡C(CH₂)₃C≡CBPin,² PinBC≡CBPin,³ Bipy•TeCl₂,⁴ and the tellurophenes **B-Te-6-B**,^{5b} **B-Te-5-B**,^{5a} **4BTe**^{5b} and **BTe**^{5b} (see below for molecular structures) were synthesized according to literature procedures. N-Iodosuccinimide (NIS) and Pd(OAc)₂ (Oakwood Chemical), Ni(dppp)Cl₂, Ni(dppe)Cl₂, and Pd(PPh₃)₄ (Strem Chemicals), 2,2'-bipyridine (GFS Organic Chemicals), and 1-bromo-4-isopropylbenzene (Matrix Scientific) were used as received without further purification. All other chemicals were purchased from Aldrich and used as received. Solutions of ¹PrMgCl•LiCl used for GRIM polymerization had their concentration determined by ¹H NMR spectrometry with 1,5-cyclooctadiene (COD) as an internal standard or via titration with a solution of I₂.^{6,7}

¹H and ¹³C{¹H} NMR spectra were collected on Varian Inova 400, 500 or 700 MHz spectrometers referenced externally to SiMe₄. Melting points were measured using a MelTemp apparatus and are reported without correction. Thermogravimetric analysis (TGA) and differential scanning calorimetry (DSC) were performed under N₂ atmosphere on a PerkinElmer Pyris 1 instrument. UV-Vis spectra were collected on a Varian Cary 300 Scan spectrometer. Gel permeation chromatography (GPC) was performed with THF (flow rate = 0.5 mL min⁻¹) using either absolute calibration with right and low angle light scattering detectors plus a refractive index detector (GPC 270 Max dual detector + Viscotek VE 3580) with a 99 kDa polystyrene standard (Malvern), or conventional calibration relative to Agilent "EasiVial" polystyrene standards (using Viscotek VE 3580), both with three Viscotek I-MBMMW-3078 columns and a Viscotek VE 2001 autosampler. The GPC analysis was accomplished via the OmniSEC 4.6 software package. Single crystal X-ray crystallography, elemental analyses and mass spectrometry (MALDI and EI-MS) were performed by the X-Ray Crystallography Laboratory, Analytical and Instrumentation Laboratory and by the Mass Spectrometry Facility, respectively, at the University of Alberta. For MALDI-MS, *trans*-2-[3-(4-*tert*-butylphenyl)-2-methyl-2-propenylidene]malononitrile (DCTB) was used as a matrix.

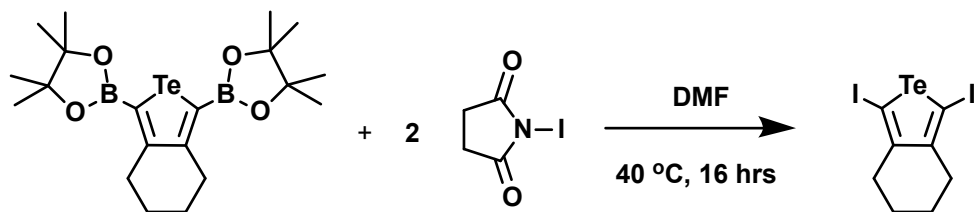
Cyclic voltammetry (CV) was performed on a CHI 660E electrochemical workstation (CH Instruments, TX, USA). The three-electrode system was assembled and tested in an Ar-filled glovebox. ITO coated glass (20 nm thick ITO, 8-10 Ω/sq, Aldrich) was used as the working

electrode. Ag wire (99.9 %, Aldrich) and Pt wire (99.9 %, BASi) were used as the pseudo-reference and counter electrode respectively. The electrolyte consisted of a 1.0 M solution of tetrabutylammonium hexafluorophosphate ($n\text{Bu}_4\text{NPF}_6$, >99.0 %) in degassed acetonitrile, and was dried over 3 Å molecular sieves prior to use. Ferrocene (98 %) was used as internal standard. The electrochemical cell consisted of a Teflon tube pressed onto an ITO substrate, which was coated with the polymer of interest. A Viton o-ring was used to provide the hermetic seal between the Teflon cell body and the working electrode. The voltage of the working electrode was scanned at 100 mV/s. Films of **PolyTe-cumenyl** and **PolyS-cumenyl** for CV measurements were drop-cast from 5 mg/mL CHCl_3 solutions followed by one hour of exposure to CHCl_3 vapor (at 35 °C) for annealing and subsequently dried under ambient conditions overnight. The same annealing procedure was used for UV-Vis and powder XRD analysis of these samples. Powder X-ray diffraction (XRD) was performed on a Rigaku Ultima IV Diffractometer by the Earth and Atmospheric Sciences' X-Ray Diffraction Laboratory at the University of Alberta.

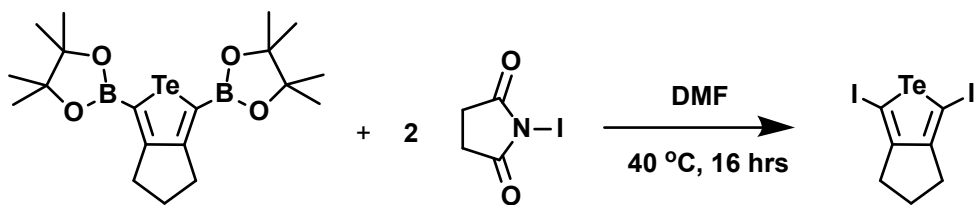
Optical HOMO-LUMO gaps (E_g) were extracted from UV-Vis by calculating the energy associated with the onset of absorption. The onset of absorption for solutions of oligomer mixtures and their films are presented in Fig. S27 and Fig. S28. For the cumenyl-substituted polymers in solution, the onset values are presented in Fig. S30 while values for films (Fig. 3) are: **PolyS-cumenyl**: 688 nm (as cast) and 698 nm (annealed); **PolyTe-cumenyl**: 956 nm (as cast or annealed – Fig. S31). To extract E_g values from cyclic voltammetry, the difference between the onset of oxidation in more positive potentials and the onset of reduction in more negative potentials was calculated. The CV onset values are shown in Fig. S46.

2. Experimental Procedures

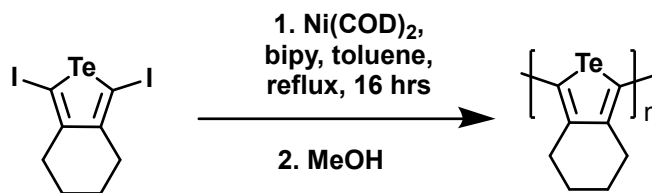
Synthesis of 1,3-diiodo-4,5,6,7-tetrahydro-benzo[c]tellurophene (I-Te-6-I): In the absence of light, **B-Te-6-B** (0.4128 g, 0.8250 mmol) and N-iodosuccinimide (0.4590 g, 2.04 mmol) were placed in a Schlenk flask and 6 mL of DMF was added. The flask was then wrapped in aluminum foil and the slurry heated to 40 °C for 16 hrs. After cooling to room temperature, 5 mL of water was then added to the mixture, creating a light-yellow slurry that was then added to 60 mL of saturated $\text{Na}_2\text{S}_2\text{O}_3$ (aq). The product was extracted with two 100 mL portions of Et_2O and the combined organic fraction was washed twice with 100 mL of water, once with 100 mL of brine, dried over MgSO_4 , and filtered. Removal of the volatiles from the filtrate *in vacuo* gave the crude **I-Te-6-I** as a brown solid. The product was then washed with three 10 mL portions of MeOH and column chromatography (silica gel, hexanes) yielded yellow, needle-like crystals (0.126 g, 31 %). Single crystals for X-ray crystallography were grown by preparing a saturated solution in hexanes and cooling it down to -30 °C. ^1H NMR (500 MHz, CDCl_3): δ 2.50-2.45 (m, 4H, I-C=CCH₂CH₂), 1.67-1.60 (m, 4H, I-C=CCH₂CH₂). $^{13}\text{C}\{^1\text{H}\}$ NMR (126 MHz, CDCl_3): δ 151.3 (I-C=C), 71.1 (I-C), 34.9 (C=CCH₂CH₂), 23.4 (C=CCH₂CH₂). HR-MS (EI) ($\text{C}_8\text{H}_8\text{I}_2\text{Te}$): m/z calcd. for $\text{C}_8\text{H}_8\text{I}_2^{130}\text{Te}$ 487.77767; found 487.77777 ($\Delta\text{ppm} = 0.2$). Anal. Calcd. for $\text{C}_8\text{H}_8\text{I}_2\text{Te}$: C 19.79, H 1.66; Found C 19.77, H 1.76. Mp (°C): 107-108 °C. UV-Vis (in THF): $\lambda_{\text{max}} = 295$ nm, $\epsilon = 7.39 \times 10^3$ L mol⁻¹ cm⁻¹.



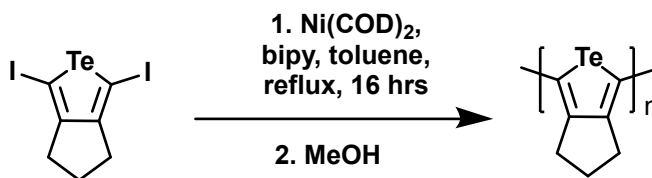
Synthesis of 1,3-diiodo-4,5,6,7-tetrahydro-cyclopenta[c]-tellurophene (I-Te-5-I): In the absence of light, **B-Te-5-B** (0.3909 g, 0.8288 mmol) and NIS (0.532 g, 2.37 mmol) were loaded into a Schlenk flask and 10 mL of DMF was added. The flask was then wrapped in aluminum foil and the slurry heated to 40 °C for 16 hrs. After cooling to room temperature, 10 mL of water was then added, creating a light-yellow slurry that was then added to 100 mL of saturated $\text{Na}_2\text{S}_2\text{O}_3$ (aq). The product was extracted with two 100 mL portions of CH_2Cl_2 and the combined organic fraction was washed twice with 200 mL of water, once with 200 mL of brine, dried over MgSO_4 , and filtered. The volatiles were removed from the filtrate *in vacuo* to afford the crude product as a brown solid. Further purification with column chromatography (silica gel, 80:1 hexanes/ CH_2Cl_2) affords **I-Te-5-I** as yellow, needle-like crystals (99 mg, 25 %). Single crystals for X-ray crystallography were grown by preparing a saturated solution in hexanes and cooling it down to -30 °C. ^1H NMR (500 MHz, CDCl_3): δ 2.60 (t, $^3J_{\text{HH}} = 7.0$ Hz, 4H, I-C=C CH_2CH_2), 2.44 (pentet, $^3J_{\text{HH}} = 7.0$ Hz, 2H, I-C=C CH_2CH_2). $^{13}\text{C}\{^1\text{H}\}$ NMR (126 MHz, CDCl_3): δ 163.5 (I-C=C), 58.9 (I-C), 35.4 (C=C CH_2CH_2), 29.0 (C=C CH_2CH_2). HR-MS (EI) ($\text{C}_7\text{H}_6\text{I}_2\text{Te}$): m/z calcd. for $\text{C}_7\text{H}_6\text{I}_2^{130}\text{Te}$ 473.76288; found 473.76215 ($\Delta\text{ppm} = 1.5$). Anal. Calcd. for $\text{C}_7\text{H}_6\text{I}_2\text{Te}$: C 17.83, H 1.28; Found C 17.87, H 1.35. Mp: 130-131 °C. UV-Vis (in THF): $\lambda_{\text{max}} = 293$ nm, $\epsilon = 7.83 \times 10^3$ L mol $^{-1}$ cm $^{-1}$.



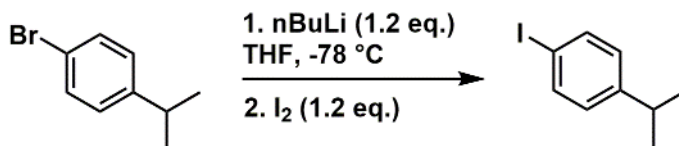
Synthesis of Oligo-Te6: $\text{Ni}(\text{COD})_2$ (0.1212 g, 0.4404 mmol) was dissolved in 3 mL of toluene to give a yellow solution. 2,2'-Bipyridine (71.3 mg, 0.457 mmol) in 3 mL of toluene was then added to form a deep purple solution. After 2 min of stirring, a solution of **I-Te-6-I** (0.1689 g, 0.3478 mmol) in 9 mL of toluene was added to give a dark brown mixture, which was heated to reflux for 16 hrs. After cooling to room temperature, the mixture was added dropwise to 300 mL of stirring MeOH under ambient conditions to precipitate **Oligo-Te6**, which was collected by suction filtration onto a cellulose thimble; this solid was purified by Soxhlet with MeOH and hexanes washes, followed by Soxhlet extraction with CHCl_3 . After drying the CHCl_3 fraction over MgSO_4 , the fraction was filtered and the volatiles were removed from the filtrate *in vacuo* to yield **Oligo-Te6** as an orange solid (42 mg, 52 %). ^1H NMR (400 MHz, CDCl_3): δ 2.67-2.41 (br, 4H, C=C CH_2CH_2), 1.64 (br, 4H, C=C CH_2CH_2). UV-Vis (in CHCl_3): $\lambda_{\text{max}} = 294$ nm, ϵ (per repeating unit) = 6.66×10^2 L mol $^{-1}$ cm $^{-1}$.



Synthesis of Oligo-Te5: Ni(COD)₂ (81.9 mg, 0.289 mmol) was dissolved in 1 mL of toluene to form a yellow solution. A solution of 2,2'-bipyridine (47.9 mg, 0.307 mmol) in 1 mL of toluene was then added to give a deep purple solution. After stirring for 2 min, a solution of **I-Te-5-I** (113.0 mg, 0.2398 mmol) in 3 mL of toluene was added and the resulting dark brown mixture was heated to reflux for 16 hrs. After cooling to room temperature, the mixture was added to 300 mL of stirring MeOH under ambient conditions to precipitate **Oligo-Te5**, which was collected by suction filtration onto a cellulose thimble; the recovered solid was purified by Soxhlet with MeOH and hexanes washes, followed by Soxhlet extraction with CHCl₃. After drying the CHCl₃ fraction over MgSO₄, the fraction was filtered and the volatiles were removed from the filtrate *in vacuo* to yield **Oligo-Te5** as a dark red solid (28 mg, 49 %). ¹H NMR (500 MHz, CDCl₃): δ 2.04 (br, 4H, C=CCH₂CH₂), 1.68 (br, 2H, C=CCH₂CH₂). UV-Vis (in CHCl₃): λ_{max} = 471 nm, ε (per repeating unit) = 5.98 x 10² L mol⁻¹ cm⁻¹.



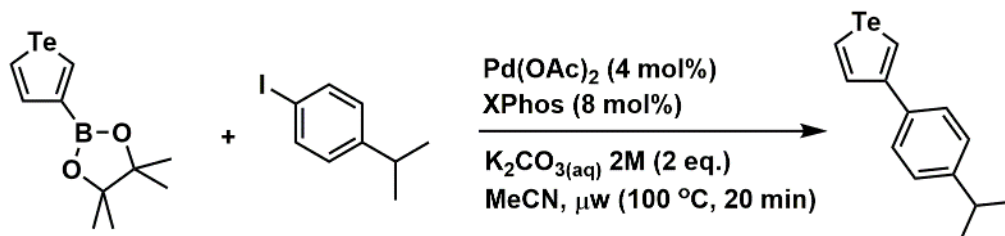
Synthesis of 1-iodo-4-isopropylbenzene: This procedure has been adapted from the literature.⁸ To a solution of 1-bromo-4-isopropylbenzene (6.0 mL, 39 mmol) in 100 mL of THF at -78 °C was added ⁿBuLi (19 mL, 2.5 M solution in hexanes, 48 mmol) dropwise, and the reaction mixture was stirred at -78 °C for 1 hr. A solution of I₂ (11.804 g, 46.507 mmol) in 50 mL of THF was then added dropwise via an addition funnel to form a dark red reaction mixture, which was then stirred for 16 hrs at room temperature. The reaction mixture was quenched by addition of 100 mL of a saturated Na₂S₂O₃ (aq). The product was then extracted with 3 x 100 mL of Et₂O, followed by washing of the combined organic layers with 3 x 100 mL of water, and drying of the organic fractions over MgSO₄. The mixture was then filtered and the volatiles were removed *in vacuo* to give a yellow oil. Further purification of the product by distillation under vacuum (*ca.* 0.2 mbar, 65 °C) afforded 1-iodo-4-isopropylbenzene as a colorless liquid (8.192 g, 86 %) with NMR data that matched literature values.⁸



Synthesis of 3-(4-cumenyl)-tellurophene (Te-cumenyl): In a glovebox, Pd(OAc)₂ (2.5 mg, 4.2 mol%) and XPhos (10.1 mg, 8.0 mol%) were added to a microwave tube along with 1.5 mL of

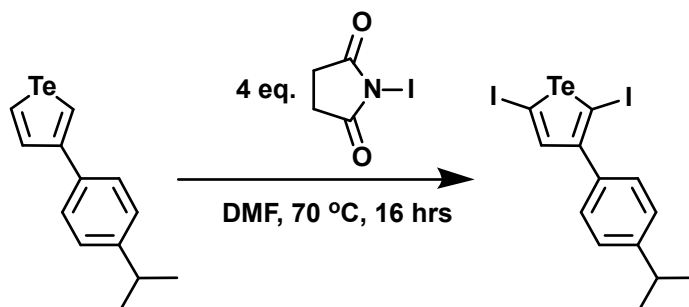
acetonitrile. The resulting suspension was stirred at room temperature until the color changed from yellow to red, at which point a solution of **BTe** (80.7 mg, 0.264 mmol) and 1-iodo-4-isopropylbenzene (75.5 mg, 0.307 mmol) in 1.5 mL of acetonitrile was added. The vial was then sealed and brought out of the glovebox for the addition of a freeze-pump-thaw degassed solution of 2.0 M K_2CO_3 (aq) (0.26 mL) via syringe through the cap. Heating under microwave irradiation at 100 °C for 20 min, followed by cooling of the mixture to room temperature, filtration of the reaction mixture through a short (*ca.* 1 cm) plug diatomaceous earth pad, and solvent removal from the filtrate *in vacuo* afforded the crude product. Purification by column chromatography (silica gel, 25:1 hexanes/ CH_2Cl_2 ; $R_f = 0.45$) yields **Te-cumenyl** as a light yellow solid (56 mg, 71 %). Single crystals for X-ray crystallography were grown by slow diffusion of a hexanes layer on top of a saturated CH_2Cl_2 solution of the product. Unreacted **BTe** (28.0 mg) could then be recovered by flushing the residual sample in the column with CH_2Cl_2 or $CHCl_3$.

Data for Te-cumenyl: 1H NMR (400 MHz, $CDCl_3$): δ 8.94 (dd, $^3J_{HH} = 6.6$, $^4J_{HH} = 1.9$ Hz, 1H, Te-CH=CH), 8.91 (t, $^4J_{HH} = 1.8$ Hz, 1H, Te-CH=C), 8.27 (dd, $^3J_{HH} = 6.6$, $^4J_{HH} = 1.6$ Hz, 1H, Te-CH=CH), 7.54 (d, $^3J_{HH} = 8.4$ Hz, 2H, *o*-ArH) 7.28 (d, $^3J_{HH} = 8.0$ Hz, 2H, *m*-ArH), 2.95 (sept, $^3J_{HH} = 6.9$ Hz, 1H, $CH(CH_3)_2$), 1.30 (d, $^3J_{HH} = 6.9$ Hz, 6H, $CH(CH_3)_2$). $^{13}C\{^1H\}$ NMR (126 MHz, $CDCl_3$): δ 152.3 (ArC), 147.9 (ArC), 138.6 (ArC), 137.5 (ArC), 127.1 (ArC), 126.8 (ArC), 125.1 (ArC), 120.0 (ArC), 34.0 ($CH(CH_3)_2$), 24.1 ($CH(CH_3)_2$). HR-MS (EI) ($C_{13}H_{14}Te$): m/z calcd. for $C_{13}H_{14}^{130}Te$ 300.01578; found 300.01637 ($\Delta ppm = 2.0$). Anal. Calcd. for $C_{13}H_{14}Te$: C 52.42, H 4.74; Found C 52.94, H 4.96. Mp: 60-62 °C.

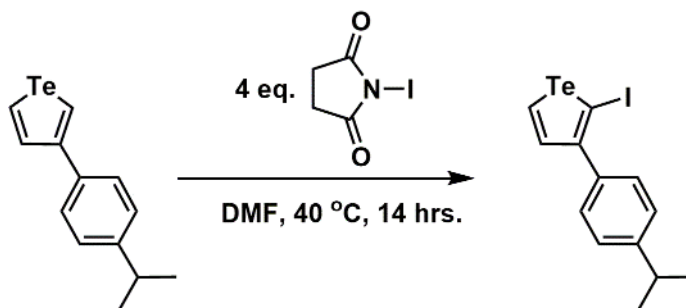


Synthesis of 2,5-diiodo-3-(4-cumenyl)-tellurophene (I-Te-cumenyl-I): In the absence of light, **Te-cumenyl** (0.260 g, 0.873 mmol) and N-iodosuccinimide (0.8227 g, 3.657 mmol) were combined in a Schlenk flask and 27 mL of DMF was added. The flask was then wrapped in aluminum foil and the mixture stirred at 70 °C for 16 hrs. The reaction mixture was then quenched by the addition of 100 mL of saturated $Na_2S_2O_3$ (aq), to give a light-yellow slurry. The product was extracted with two 100 mL portions of CH_2Cl_2 , and the volume of the combined extracts was reduced to 75 mL *in vacuo*. The resulting solution was washed four times with 100 mL of water and once with 100 mL of brine. After drying the organic phase over $MgSO_4$, the mixture was filtered and the volatiles were removed from the filtrate *in vacuo* to give crude **I-Te-cumenyl-I** (0.424 g, 88 %) as an oil. Although mono-iodinated tellurophene impurities elute very close to the product, purification by repeating three column chromatographic separations in a row (silica gel, hexanes) to remove trace quantities (*ca.* 4-8 %) of the mono-iodinated product (**H-Tecumenyl-I**) from the crude product to give analytically pure **I-Te-cumenyl-I** as an orange oil (0.274 g, 57 %). 1H NMR (400 MHz, $CDCl_3$): δ 7.93 (s, 1H, Te-C(I)=CH), 7.33 – 7.25 (m, 4H, ArH), 2.96 (sept, $^3J_{HH} = 7.0$ Hz, 1H, $CH(CH_3)_2$), 1.30 (d, $^3J_{HH} = 6.9$ Hz, 6H, $CH(CH_3)_2$). $^{13}C\{^1H\}$ NMR (101 MHz, $CDCl_3$): δ 157.8 (ArC), 149.8 (ArC), 148.7 (ArC), 136.3 (ArC), 129.0 (ArC), 126.4

(ArC), 70.7 (C-I), 70.0 (C-I), 34.1 (CH(CH₃)₂), 24.1 (CH(CH₃)₂). HR-MS (EI) (C₁₃H₁₂I₂Te): m/z calcd. for C₁₃H₁₂¹³⁰TeI₂ 551.80908; found 551.80898 (Δ ppm = 0.2). Anal. Calcd. for C₁₃H₁₂I₂Te: C 28.41, H 2.20; Found C 28.56, H 2.26. UV-Vis (in THF): λ_{max} = 242 nm, ϵ = 2.35 x 10⁴ L mol⁻¹ cm⁻¹; λ_{max} = 299 nm, ϵ = 2.01 x 10⁴ L mol⁻¹ cm⁻¹.

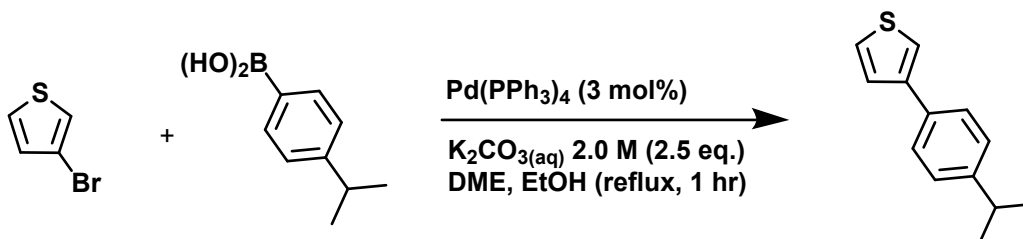


Synthesis of 2-iodo-3-(4-cumenyl)-tellurophene (H-Te-cumenyl-I): In the absence of light, **Te-cumenyl** (0.0551 g, 0.1850 mmol) and N-iodosuccinimide (0.0874 g, 0.3885 mmol) were combined in a Schlenk flask and 4 mL of DMF was added. The flask was then wrapped in aluminum foil and the mixture stirred at 40 °C for 14 hrs. The reaction mixture was then allowed to cool to room temperature and quenched by the addition of 80 mL of saturated Na₂S₂O₃ (aq), to give a light-yellow slurry. The product was extracted with two 100 mL portions of CH₂Cl₂ and the combined organic fractions were washed twice with 130 mL of brine. After drying the organic phase over MgSO₄, the mixture was filtered and the volatiles were removed from the filtrate *in vacuo* to give crude **H-Te-cumenyl-I** as a yellow oil (0.080 g, 87 % of **H-Te-cumenyl-I** and 13% of **I-Te-cumenyl-I**, as determined by ¹H NMR). **Data for H-Te-cumenyl-I:** ¹H NMR (700 MHz, CDCl₃): δ 9.02 (d, ³J_{HH} = 7.1 Hz, 1H, Te-CH=CH), 7.63 (d, ³J_{HH} = 7.7 Hz, 1H, Te-CH=CH), 7.64 – 7.28 (m, 4H, ArH), 2.96 (sept, ³J_{HH} = 6.3 Hz, 1H, CH(CH₃)₂), 1.29 (d, ³J_{HH} = 7.0 Hz, 6H, CH(CH₃)₂). ¹³C{¹H} NMR (176 MHz, CDCl₃): δ 156.6 (ArC), 148.3 (ArC), 140.2 (ArC), 137.8 (ArC), 130.2 (ArC), 129.0 (ArC), 126.4 (ArC), 66.3 (C-I), 34.1 (CH(CH₃)₂), 24.1 (CH(CH₃)₂). HR-MS (EI) (C₁₃H₁₃I¹³⁰Te): m/z calcd. for C₁₃H₁₃I¹³⁰Te 425.91245; found 425.91290 (Δ ppm = 1.1).

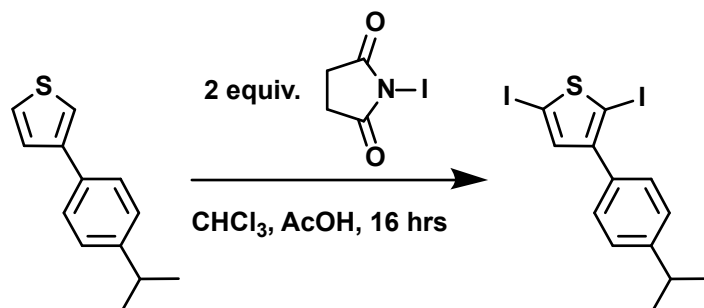


Synthesis of 3-(4-cumenyl)-thiophene (S-cumenyl): This procedure was adapted from the literature.⁹ Pd(PPh₃)₄ (0.3522 g, 0.3048 mmol) was loaded into a Schlenk flask and 20 mL of N₂-sparged 1,2-dimethoxyethane was added, followed by 3-bromothiophene (1.00 mL, 10.7 mmol) and freeze-pump-thaw degassed 2.0 M K₂CO₃ (aq) (13 mL). The mixture was stirred at room temperature for 10 min and then a solution of 4-isopropylphenylboronic acid (2.137 g, 13.03

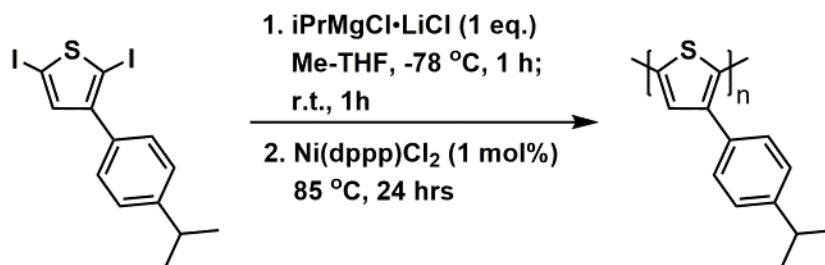
mmol) in 20 mL of N₂-sparged anhydrous EtOH was added. The mixture was heated to reflux for 1 hr and then allowed to cool to room temperature with additional stirring for 16 hrs. Filtration of the mixture through a *ca.* 1 cm plug of diatomaceous earth followed by solvent removal from the filtrate. Column chromatography (silica gel, hexanes) afforded **S-cumenyl** as a white solid (2.074 g, 97 %). ¹H NMR (500 MHz, CDCl₃) δ 7.53 (d, ³J_{HH} = 8.3 Hz, 2H, *o*-ArH), 7.45 – 7.35 (m, 3H, ArH thienyl), 7.30 – 7.21 (d, ³J_{HH} = 8.0 Hz, 2H, *m*-ArH), 2.94 (sept, ³J_{HH} = 6.9 Hz, 1H, CH(CH₃)₂), 1.28 (d, ³J_{HH} = 6.9 Hz, 6H, CH(CH₃)₂). ¹³C{¹H} NMR (126 MHz, CDCl₃): δ 148.0 (ArC), 142.5 (ArC), 133.7 (ArC), 127.0 (ArC), 126.6 (ArC), 126.5 (ArC), 126.1 (ArC), 119.9 (ArC), 34.0 (CH(CH₃)₂), 24.1 (CH(CH₃)₂). HR-MS (EI) (C₁₃H₁₄S): *m/z* calcd. 202.08162; found 202.08187 (Δppm = 1.2). Anal. Calcd. for C₁₃H₁₄S: C 77.18, H 6.98, S 15.85; found C 78.14, H 7.08, S 14.39. Mp: 62-63 °C.



Synthesis of 2,5-diiodo-3-(4-cumenyl)-thiophene (I-S-cumenyl-I): Procedure adapted from the literature.¹⁰ In the absence of light, N-iodosuccinimide (0.523 g, 2.32 mmol) and **S-cumenyl** (0.196 g, 0.969 mmol) were loaded into a Schlenk flask that was wrapped in aluminum foil. An N₂-sparged mixture of CHCl₃ (5 mL) and AcOH (5 mL) was added and the mixture stirred at room temperature for 16 hrs. Saturated Na₂S₂O₃ (aq) was added until the mixture turned yellow. The resulting mixture was added to water (20 mL) and extracted with two portions of CH₂Cl₂ (20 mL). The combined organic fractions were washed with water (20 mL) and brine (20 mL), and the dried over MgSO₄. Filtration of the mixture followed by removal of the solvent from the filtrate gave a crude product that was further purified by column chromatography (silica gel, hexanes) to afford **I-S-cumenyl-I** as a light yellow oil (0.360 g, 82 %). ¹H NMR (400 MHz, CDCl₃): δ 7.40 (d, ³J_{HH} = 8.2 Hz, 2H, *o*-ArH), 7.30 (d, ³J_{HH} = 8.2 Hz, 2H, *m*-ArH), 7.10 (s, 1H, S-C(I)=CH), 2.98 (sept, ³J_{HH} = 6.9 Hz, 1H, CH(CH₃)₂), 1.32 (d, ³J_{HH} = 7.0 Hz, 6H, CH(CH₃)₂). ¹³C{¹H} NMR (101 MHz, CDCl₃): δ 148.9 (ArC), 148.9 (ArC), 138.8 (ArC), 132.8 (ArC), 128.7 (ArC), 126.6 (ArC), 77.0 (C-I), 75.9 (C-I), 34.0 (CH(CH₃)₂), 24.1 (CH(CH₃)₂). HR-MS (EI) (C₁₃H₁₂SI₂): *m/z* calcd. 453.87494; found 453.87516 (Δppm = 0.5). Anal. Calcd. for C₁₃H₁₂SI₂: C 34.38, H 2.66, S 7.06; found C 35.22, H 2.68, S 7.14. UV-Vis (in THF): λ_{max} = 245 nm, ε = 2.97 x 10⁴ L mol⁻¹ cm⁻¹; λ_{max} = 270 nm, ε = 1.34 x 10⁴ L mol⁻¹ cm⁻¹.

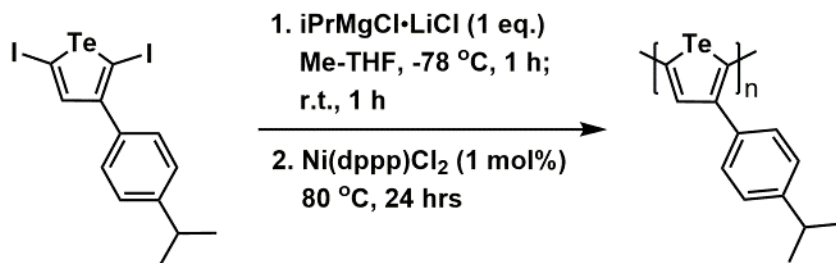


Synthesis of poly(3-(4-cumenyl)-thiophene) (PolyS-cumenyl): To a mixture of **I-S-cumenyl-I** (0.3500 g, 0.7707 mmol) and Me-THF (6 mL) cooled to $-78\text{ }^{\circ}\text{C}$ was added dropwise a solution of $i\text{PrMgCl}\cdot\text{LiCl}$ (0.77 mmol; 1.3 M solution in THF). The mixture was stirred at $-78\text{ }^{\circ}\text{C}$ for 1 hr followed by stirring at room temperature for 1 hr. The mixture was then transferred to a Teflon-capped Schlenk flask containing $\text{Ni}(\text{dppp})\text{Cl}_2$ (0.0042 g, 1.0 mol%) and stirred at $80\text{ }^{\circ}\text{C}$ for 1 day. The reaction mixture was quenched by addition of 2.0 mL of 1.2 M HCl (aq); the resulting mixture was then added dropwise to 300 mL of stirring acetone (cooled to $-30\text{ }^{\circ}\text{C}$) to precipitate the polymer, followed by polymer isolation by suction filtration onto a cellulose thimble. The isolated polymer was then purified by subsequent Soxhlet washings with MeOH and hexanes and recovered by Soxhlet extraction with CHCl_3 ; removal of the solvent from the CHCl_3 extract afforded **PolyS-cumenyl** as a dark purple solid (58.8 mg, 39 %). ^1H NMR (500 MHz, CDCl_3): δ 7.49 – 7.02 (br, 4H, ArH), 6.99 – 6.67 (br, 1H, S-C=CH), 2.94 (br sept, $^3J_{\text{HH}} = 7.0$ Hz, 1H, $\text{CH}(\text{CH}_3)_2$), 1.28 (br d, $^3J_{\text{HH}} = 6.6$ Hz, 6H, $\text{CH}(\text{CH}_3)_2$). $M_w = 12$ kDa (absolute) or 8.5 kDa (relative to polystyrene standards), PDI = 1.1. $T_g = 176\text{ }^{\circ}\text{C}$ (by DSC). UV-Vis (in THF): $\lambda_{\text{max}} = 275$ nm, ϵ (per repeating unit) = 3.09×10^3 L mol $^{-1}$ cm $^{-1}$; $\lambda_{\text{max}} = 455$ nm, ϵ (per repeating unit) = 3.00×10^3 L mol $^{-1}$ cm $^{-1}$.



Synthesis of poly(3-(4-cumenyl)-tellurophene) (PolyTe-cumenyl): To a solution of **I-Te-cumenyl-I** (0.1943 g, 0.3535 mmol) in 2.7 mL of Me-THF at $-78\text{ }^{\circ}\text{C}$ was added a solution of $i\text{PrMgCl}\cdot\text{LiCl}$ (0.35 mmol; 1.4 M solution in THF) dropwise. The mixture was stirred at $-78\text{ }^{\circ}\text{C}$ for 1 hr followed by stirring at room temperature for another 1 hr. The mixture was then transferred to a Teflon-capped Schlenk flask containing $\text{Ni}(\text{dppp})\text{Cl}_2$ (0.0019 g, 1.0 mol%) and the mixture stirred at $80\text{ }^{\circ}\text{C}$ for 1 day. The reaction mixture was quenched by addition of 1.0 mL of 1.2 M HCl (aq); the resulting mixture was then added dropwise to 300 mL of stirring acetone (cooled to $-30\text{ }^{\circ}\text{C}$) to precipitate the polymer, followed by polymer isolation by suction filtration onto a cellulose thimble. The collected polymer was then purified by subsequent Soxhlet washings with MeOH and hexanes and recovered by Soxhlet extraction with CHCl_3 ; removal of the solvent from the CHCl_3 extract afforded **PolyTe-cumenyl** as a dark blue-purple solid (24.0

mg, 23 %). ^1H NMR (500 MHz, CDCl_3) δ 7.52 – 6.81 (br m, 5H, ArH and Te-C=CH), 3.07 – 2.80 (br m, 1H, $\text{CH}(\text{CH}_3)_2$), 1.28 (br, 6H, $\text{CH}(\text{CH}_3)_2$). M_w = 5.8 kDa (relative to polystyrene standards), PDI = 1.1. If we assume that **PolyTe-cumenyl** behaves similarly to **PolyS-cumenyl** in the GPC column, we can multiply its M_w relative to polystyrene by 1.41 (ratio of $M_w^{\text{absolute}}/M_w^{\text{relative}}$ for **PolyS-cumenyl**) to obtain an estimated absolute M_w of 8.2 kDa. UV-Vis (in THF): λ_{max} = 267 nm, ϵ (per repeating unit) = $4.53 \times 10^3 \text{ L mol}^{-1} \text{ cm}^{-1}$; $\lambda_{\text{shoulder}}$ = 372 nm; λ_{max} = 607 nm, ϵ (per repeating unit) = $4.66 \times 10^3 \text{ L mol}^{-1} \text{ cm}^{-1}$.



Polymerization Trials using $\text{Ni}(\text{dppe})\text{Cl}_2$ as a Pre-catalyst

Synthesis of poly(3-(4-cumenyl)-thiophene) (PolyS-cumenyl) with $\text{Ni}(\text{dppe})\text{Cl}_2$ at $80\text{ }^\circ\text{C}$: To a mixture of **I-S-cumenyl-I** (0.1502 g, 0.3307 mmol) and Me-THF (2.6 mL) cooled to $-78\text{ }^\circ\text{C}$ was added dropwise a solution of $i\text{PrMgCl}\cdot\text{LiCl}$ (0.33 mmol; 0.56 M solution in THF). The mixture was stirred at $-78\text{ }^\circ\text{C}$ for 1 hr followed by stirring at room temperature for 1 hr. The mixture was then transferred to a Teflon-capped Schlenk flask containing $\text{Ni}(\text{dppe})\text{Cl}_2$ (0.0018 g, 1.0 mol%) and stirred at $80\text{ }^\circ\text{C}$ for 1 day. The reaction mixture was quenched by addition of 1.0 mL of 1.2 M HCl (aq); the resulting mixture was then added dropwise to 300 mL of stirring MeOH (cooled to $-30\text{ }^\circ\text{C}$) to precipitate the polymer, followed by isolation by suction filtration onto a cellulose thimble. The isolated polymer was then purified by subsequent Soxhlet washings with MeOH and hexanes and recovered by Soxhlet extraction with CHCl_3 ; removal of the solvent from the CHCl_3 extract afforded **PolyS-cumenyl** as a dark purple solid (7.2 mg, 11 %). Regioregularity = 88 %, M_w = 6.1 kDa (absolute), PDI = 1.1. Additionally, a large amount of crude orange solid was recovered in the hexanes fraction (40 mg, 60 %, M_w = 13 kDa (absolute), PDI = 1.1) corresponding to polythiophene of lower regioregularity (65 %, as determined by ^1H NMR).

Synthesis of poly(3-(4-cumenyl)-tellurophene) (PolyTe-cumenyl) with $\text{Ni}(\text{dppe})\text{Cl}_2$ at $80\text{ }^\circ\text{C}$: To a solution of **I-Te-cumenyl-I** (0.1733 g, 0.3153 mmol) in 2.4 mL of Me-THF at $-78\text{ }^\circ\text{C}$ was added a solution of $i\text{PrMgCl}\cdot\text{LiCl}$ (0.35 mmol; 0.56 M solution in THF) dropwise. The mixture was stirred at $-78\text{ }^\circ\text{C}$ for 1 hr followed by stirring at room temperature for 1 hr. The mixture was then transferred to a Teflon-capped Schlenk flask containing $\text{Ni}(\text{dppe})\text{Cl}_2$ (0.0017 g, 1.0 mol%) and the mixture stirred at $80\text{ }^\circ\text{C}$ for 1 day. The reaction mixture was quenched by addition of 1.0 mL of 1.2 M HCl (aq); the resulting mixture was then added dropwise to 300 mL of stirring MeOH (cooled to $-30\text{ }^\circ\text{C}$) to precipitate the polymer, followed by isolation by suction filtration onto a cellulose thimble. The collected polymer was then purified by subsequent Soxhlet washings with MeOH and hexanes and recovered by Soxhlet extraction with CHCl_3 ; removal of the solvent from the CHCl_3 extract afforded minimal **PolyTe-cumenyl** as a dark purple solid (< 1 mg, 1 %) that could not be characterized by NMR spectroscopy or GPC. Most of the product was

recovered in the hexanes fraction (from Soxhlet) as a crude red-purple solid (24 mg, 26 %, $M_w = 2.5$ kDa (absolute), PDI = 1.5) and red-shifted absorption of $\lambda_{\max} = 495$ nm in THF.

Synthesis of poly(3-(4-cumenyl)-tellurophene) (PolyTe-cumenyl) with Ni(dppe)Cl₂ at 40 °C: To a solution of **I-Te-cumenyl-I** (0.0558 g, 0.1015 mmol) in 0.77 mL of Me-THF at -78 °C was added a solution of *i*PrMgCl•LiCl (0.10 mmol; 0.56 M solution in THF) dropwise. The mixture was stirred at -78 °C for 1 hr followed by stirring at room temperature for 1 hr. The mixture was then transferred to a Teflon-capped Schlenk flask containing Ni(dppe)Cl₂ (0.0006 g, 1.1 mol%) and the mixture stirred at 40 °C for 1 day. The reaction mixture was quenched by addition of 1.0 mL of 1.2 M HCl (aq); the resulting mixture was then added dropwise to 300 mL of stirring MeOH (cooled to -30 °C) to precipitate the polymer, followed by isolation by suction filtration onto a cellulose thimble. The collected polymer was then purified by subsequent Soxhlet washings with MeOH and hexanes and recovered by Soxhlet extraction with CHCl₃; removal of the solvent from the CHCl₃ extract afforded **PolyTe-cumenyl** as a dark blue-purple solid (4.0 mg, 13 %). Regioregularity = 73 % (determined by ¹H NMR), $M_w = 2.9$ kDa (relative to polystyrene standards), $M_w = 4.1$ kDa (estimated absolute), PDI = 1.5.

3. DFT Computations

Computational details: Gas-phase structure optimization was performed using density functional theory (DFT) with the B3LYP functional^{11,12} and the basis sets 6-31G(d,p), for C, H and S,^{13,14} and LANL2DZ, for Te and I.¹⁵ Computations were performed with the Gaussian09 or Gaussian16 software and frequency analysis confirmed all structures to be in local minima on the potential energy surface.^{16,17} The structures and orbitals are shown as visualized in Avogadro.¹⁸ As a starting point for the computation of oligomers, the chains were built by linking monomer structures determined by single crystal XRD, which were then optimized. The average dihedral (torsional) angle between tellurophene units of **Oligo-Te6** and **Oligo-Te5** remained the same for optimizations with 3-, 5- or 7-units in the oligomeric chain. For the calculation of energy change with torsion angle (Fig. S2), the respective structures were optimized with a fixed dihedral angle.

For time dependent calculations (TD-DFT), trimers were used for simplicity using the same level of theory as stated above. The three strongest oscillators at their respective wavenumbers were used to calculate absorptivity and to build the computational UV-Vis spectra. Using all calculated oscillators leads to a very similar absorption profile and the same conclusion of a red-shifted absorption for **Oligo-Te5**, as supported by experiment.

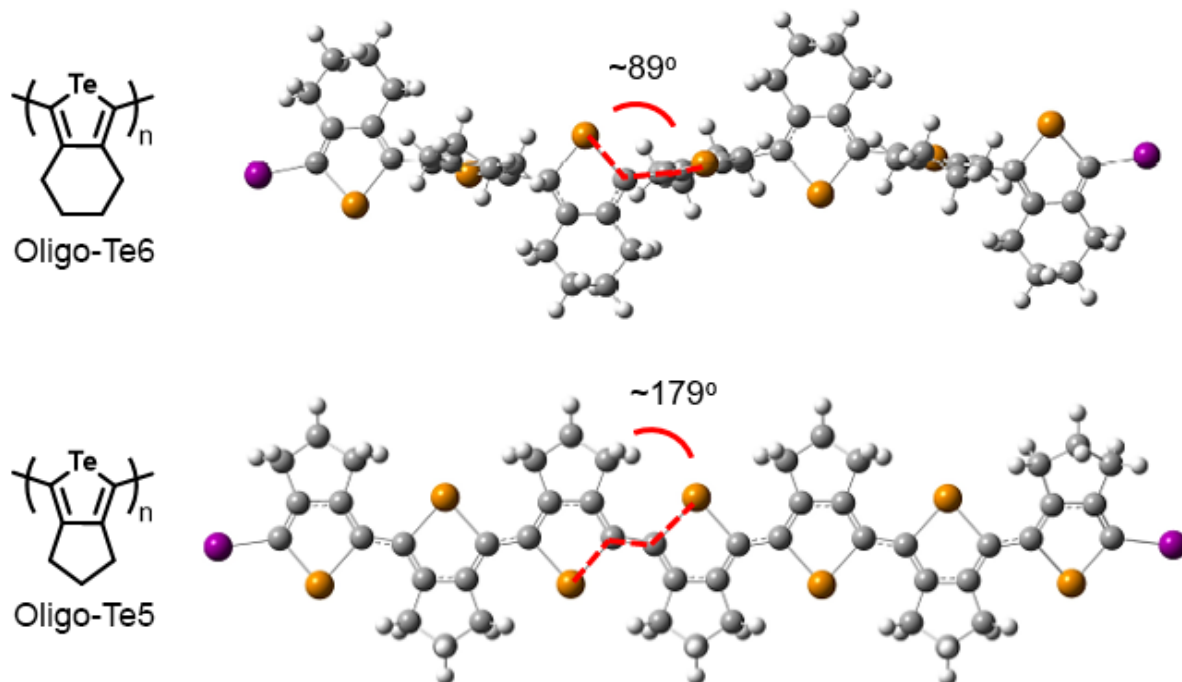


Fig. S1. Structure optimization of heptamers of **Oligo-Te6** and **Oligo-Te5**. The average torsional angle for the oligomers is highlighted in the Figure.

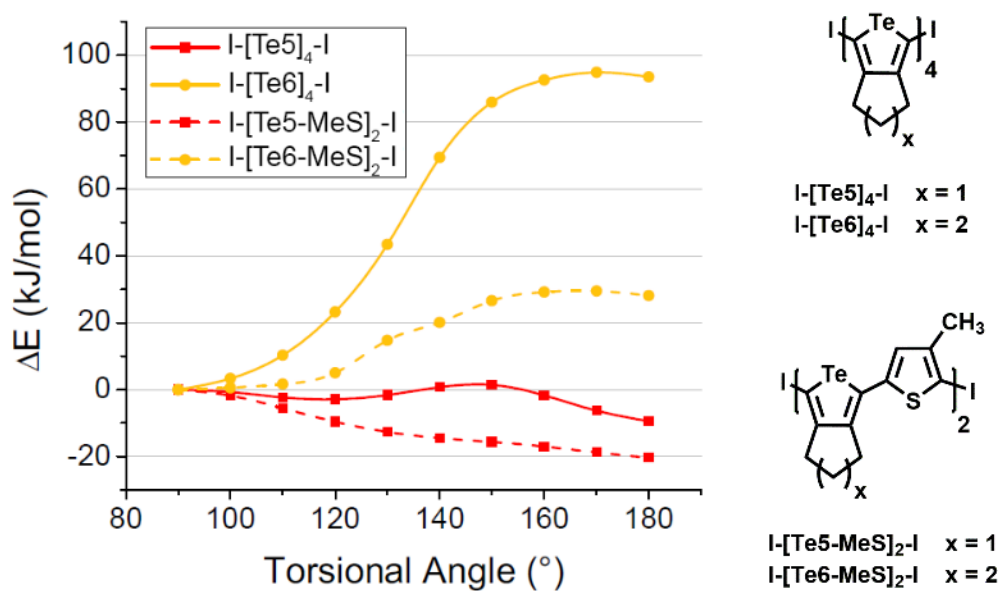


Fig. S2. Energy change of oligomers upon change in torsional angle between the chalcogenophene rings. The energy is calculated relative to the 90° position for tetrameric models of oligomers terminated by iodine consisting of four units of each tellurophene ($I-[Te6]_4-I$ and $I-[Te5]_4-I$) or a copolymer of same length with 3-methylthiophene ($I-[Te6-MeS]_2-I$ and $I-[Te5-MeS]_2-I$).

Table S1. Computed excited states of trimers of **Oligo-Te5 (I-[Te5]₃-I)** and **Oligo-Te6 (I-[Te6]₃-I)** by TD-DFT. The three strongest oscillators are shown in bold and the main orbitals involved in singlet state transitions are shown.

| I-[Te5] ₃ -I | | | | I-[Te6] ₃ -I | | | |
|-------------------------|-------------|---------------------|----------------------------|-------------------------|-------------|---------------------|------------------------|
| Excited state | Energy (eV) | Oscillator strength | Main orbitals involved | Excited state | Energy (eV) | Oscillator strength | Main orbitals involved |
| T ₁ | 1.5346 | 0.0000 | | T ₁ | 2.5546 | 0.0000 | |
| T ₂ | 2.5209 | 0.0000 | | T ₂ | 2.6745 | 0.0000 | |
| S ₁ | 2.8119 | 0.9915 | HOMO/LUMO | T ₃ | 2.6803 | 0.0000 | |
| T ₃ | 2.8138 | 0.0000 | | T ₄ | 3.1543 | 0.0000 | |
| T ₄ | 2.8920 | 0.0000 | | T ₅ | 3.1628 | 0.0000 | |
| S ₂ | 2.9745 | 0.0003 | HOMO/LUMO+1 | T ₆ | 3.1863 | 0.0000 | |
| T ₅ | 2.9780 | 0.0000 | | T ₇ | 3.1936 | 0.0000 | |
| T ₆ | 2.9899 | 0.0000 | | T ₈ | 3.2390 | 0.0000 | |
| T ₇ | 3.0015 | 0.0000 | | T ₉ | 3.2909 | 0.0000 | |
| S ₃ | 3.0894 | 0.0001 | HOMO/LUMO+2 HOMO/LUMO+3 | T ₁₀ | 3.4031 | 0.0000 | |
| T ₈ | 3.1421 | 0.0000 | | S ₁ | 3.4634 | 0.0007 | HOMO/LUMO |
| S ₄ | 3.1665 | 0.0004 | HOMO/LUMO+2 HOMO/LUMO+3 | S ₂ | 3.5199 | 0.0003 | HOMO/LUMO+2 |
| T ₉ | 3.1688 | 0.0000 | | S ₃ | 3.5862 | 0.0032 | HOMO-2/LUMO |
| S ₅ | 3.2455 | 0.0001 | HOMO/LUMO+4 | S ₄ | 3.6065 | 0.0008 | HOMO-4/LUMO |
| T ₁₀ | 3.3096 | 0.0000 | | S ₅ | 3.6264 | 0.0022 | HOMO-1/LUMO+3 |
| S ₆ | 3.5047 | 0.0479 | HOMO-1/LUMO | S ₆ | 3.6280 | 0.0004 | HOMO/LUMO+2 |
| S ₇ | 3.6234 | 0.0005 | HOMO/LUMO+6 | S ₇ | 3.6770 | 0.0001 | HOMO-2/LUMO+3 |
| S ₈ | 3.6413 | 0.0030 | HOMO-2/LUMO | S ₈ | 3.7612 | 0.0001 | HOMO-3/LUMO |
| S ₉ | 3.6581 | 0.0002 | HOMO/LUMO+5 | S ₉ | 3.8135 | 0.0154 | HOMO-2/LUMO |
| S ₁₀ | 3.6764 | 0.0191 | HOMO-3/LUMO | S ₁₀ | 3.8601 | 0.0717 | HOMO-1/LUMO |

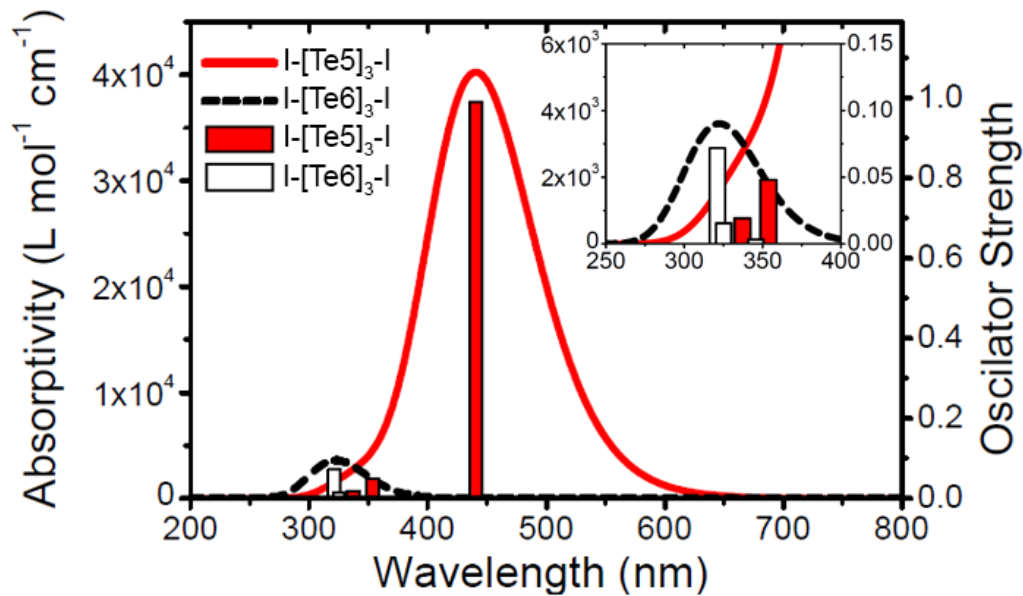


Fig. S3. Computed UV-Vis absorptivity for trimers of **Oligo-Te5 (I-[Te5]₃-I)** and **Oligo-Te6 (I-[Te6]₃-I)** and the three main oscillator strengths (bars below the curves) associated with the absorptions. The inset shows an expansion of the short wavelength region.

4. X-Ray Crystallography

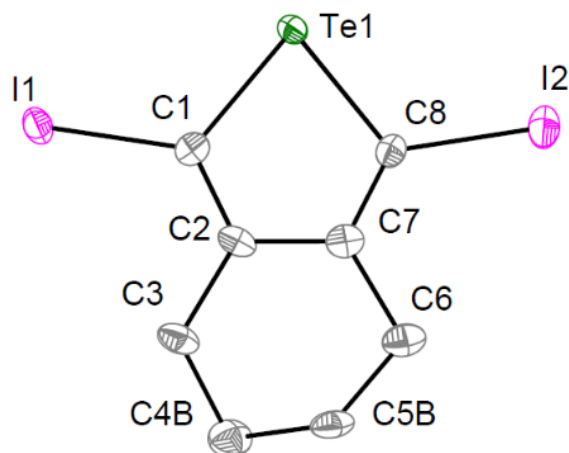


Fig. S4. Molecular structure of 1,3-diiodo-4,5,6,7-tetrahydro-benzo[c]tellurophene (**I-Te-6-I**). Thermal ellipsoids plotted at a 30 % probability level with hydrogen atoms omitted for clarity. Selected bond lengths (Å) and angle (°): Te1-C1 2.080(3), Te1-C8 2.090(3), I1-C1 2.079(2), I2-C8 2.083(3); C1-Te1-C8 80.92(11).

Table S2. Crystallographic experimental details for 1,3-diiodo-4,5,6,7-tetrahydro-benzo[c]-tellurophene (**I-Te-6-I**).

A. Crystal Data

| | |
|--|--|
| formula | C ₈ H ₈ I ₂ Te |
| formula weight | 485.54 |
| crystal dimensions (mm) | 0.58 × 0.06 × 0.06 |
| crystal system | monoclinic |
| space group | <i>P</i> 2 ₁ / <i>n</i> (an alternate setting of <i>P</i> 2 ₁ / <i>c</i> [No. 14]) |
| unit cell parameters ^a | |
| <i>a</i> (Å) | 22.122 (5) |
| <i>b</i> (Å) | 4.6531 (12) |
| <i>c</i> (Å) | 22.137 (5) |
| β (deg) | 108.971 (3) |
| <i>V</i> (Å ³) | 2154.9 (9) |
| <i>Z</i> | 8 |
| ρ _{calcd} (g cm ⁻³) | 2.993 |
| μ (mm ⁻¹) | 8.433 |

Table S2 (con't):**B. Data Collection and Refinement Conditions**

| | |
|--|--|
| diffractometer | Bruker D8/APEX II CCD ^b |
| radiation (λ [Å]) | graphite-monochromated Mo K α (0.71073) |
| temperature (°C) | −100 |
| scan type | ω scans (0.3°) (20 s exposures) |
| data collection 2θ limit (deg) | 53.46 |
| total data collected | 14132 ($-27 \leq h \leq 27$, $-5 \leq k \leq 5$, $-28 \leq l \leq 27$) |
| independent reflections | 4556 ($R_{\text{int}} = 0.0361$) |
| number of observed reflections (<i>NO</i>) | 3959 [$F_o^2 \geq 2\sigma(F_o^2)$] |
| structure solution method | intrinsic phasing (<i>SHELXT-2014</i> ^c) |
| refinement method | full-matrix least-squares on F^2 (<i>SHELXL-2014</i> ^{d,e}) |
| absorption correction method | Gaussian integration (face-indexed) |
| range of transmission factors | 0.7660–0.0469 |
| data/restraints/parameters | 4556 / 90 ^f / 236 |
| goodness-of-fit (<i>S</i>) ^g [all data] | 1.067 |
| final <i>R</i> indices ^h | |
| R_1 [$F_o^2 \geq 2\sigma(F_o^2)$] | 0.0380 |
| wR_2 [all data] | 0.0922 |
| largest difference peak and hole | 3.394 and −0.697 e Å ^{−3} |

^aObtained from least-squares refinement of 5968 reflections with $4.52^\circ < 2\theta < 53.22^\circ$.

^bPrograms for diffractometer operation, data collection, data reduction and absorption correction were those supplied by Bruker.

^cSheldrick, G. M. *Acta Crystallogr.* **2015**, *A71*, 3–8. (*SHELXT-2014*)

^dSheldrick, G. M. *Acta Crystallogr.* **2015**, *C71*, 3–8. (*SHELXL-2014*)

^eThe data were tested for nonmerohedral twinning using the TwinRotMat procedure as implemented in *PLATON* (Spek, A. L. *Acta Crystallogr.* **1990**, *A46*, C34; Spek, A. L. *J. Appl. Cryst.* **2003**, *36*, 7–13. *PLATON* - a multipurpose crystallographic tool. Utrecht University, Utrecht, The Netherlands). The second twin component can be related to the first component by twofold rotation about the [1 0 −1] axis (twin law [0 0 −1 0 −1 0 −1 0 0]). The refined value of the twin fraction (*SHELXL-2014* BASF parameter) was 0.4360(14).

^fThe C–C distances involving the disordered aliphatic backbone were restrained to be approximately the same by use of the *SHELXL SADI* instruction. Likewise, the anisotropic displacement parameters of the disordered groups had a rigid-bond restraint applied (*SHELXL RIGU* instruction).

^g $S = [\sum w(F_o^2 - F_c^2)^2 / (n - p)]^{1/2}$ (n = number of data; p = number of parameters varied; $w = [\sigma^2(F_o^2) + (0.0528P)^2]^{-1}$ where $P = [\text{Max}(F_o^2, 0) + 2F_c^2]/3$).

^h $R_1 = \sum ||F_o| - |F_c|| / \sum |F_o|$; $wR_2 = [\sum w(F_o^2 - F_c^2)^2 / \sum w(F_o^4)]^{1/2}$.

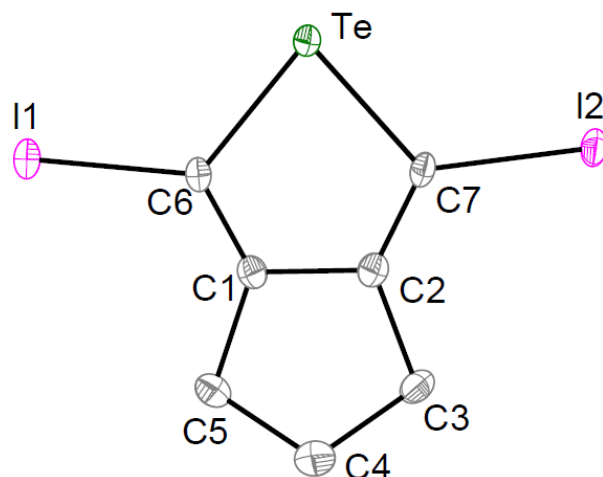


Fig. S5. Molecular structure of 1,3-diiodo-4,5,6,7-tetrahydro-cyclopenta[*c*]-tellurophene (**I-Te-5-I**). Thermal ellipsoids plotted at a 30 % probability level with hydrogen atoms omitted for clarity. Selected bond lengths (Å) and angle (°): Te-C6 2.076(9), Te-C7 2.080(10), I1-C6 2.062(9), I2-C7 2.081(10); C6-Te-C7 79.2(4).

Table S3. Crystallographic experimental details for 1,3-diiodo-4,5,6,7-tetrahydro-cyclopenta[*c*]-tellurophene (**I-Te-5-I**)

A. Crystal Data

| | |
|--|--|
| formula | C ₇ H ₆ I ₂ Te |
| formula weight | 471.52 |
| crystal dimensions (mm) | 0.42 × 0.16 × 0.05 |
| crystal system | monoclinic |
| space group | <i>P</i> 2 ₁ / <i>n</i> (an alternate setting of <i>P</i> 2 ₁ / <i>c</i> [No. 14]) |
| unit cell parameters ^a | |
| <i>a</i> (Å) | 12.4859 (6) |
| <i>b</i> (Å) | 4.5525 (2) |
| <i>c</i> (Å) | 17.4405 (8) |
| β (deg) | 100.5674 (5) |
| <i>V</i> (Å ³) | 974.54 (8) |
| <i>Z</i> | 4 |
| ρ _{calcd} (g cm ⁻³) | 3.214 |
| μ (mm ⁻¹) | 9.319 |

Table S3 (con't):**B. Data Collection and Refinement Conditions**

| | |
|---|---|
| diffractometer | Bruker D8/APEX II CCD ^b |
| radiation (λ [Å]) | graphite-monochromated Mo K α (0.71073) |
| temperature (°C) | –100 |
| scan type | ω scans (0.3°) (10 s exposures) |
| data collection 2θ limit (deg) | 56.73 |
| total data collected | 8738 ($-16 \leq h \leq 16$, $-6 \leq k \leq 6$, $-23 \leq l \leq 23$) |
| independent reflections | 2413 ($R_{\text{int}} = 0.0143$) |
| number of observed reflections (NO) | 2278 [$F_o^2 \geq 2\sigma(F_o^2)$] |
| structure solution method | Patterson/structure expansion (DIRDIF–2008 ^c) |
| refinement method | full-matrix least-squares on F^2 (SHELXL–2014 ^d) |
| absorption correction method | Gaussian integration (face-indexed) |
| range of transmission factors | 0.7025–0.1288 |
| data/restraints/parameters | 2413 / 0 / 91 |
| goodness-of-fit (S) ^e [all data] | 1.159 |
| final R indices ^f | |
| R_1 [$F_o^2 \geq 2\sigma(F_o^2)$] | 0.0184 |
| wR_2 [all data] | 0.0428 |
| largest difference peak and hole | 0.512 and –0.836 e Å ^{–3} |

^aObtained from least-squares refinement of 9982 reflections with $4.42^\circ < 2\theta < 56.70^\circ$.

^bPrograms for diffractometer operation, data collection, data reduction and absorption correction were those supplied by Bruker.

^cBeurskens, P. T.; Beurskens, G.; de Gelder, R.; Smits, J. M. M.; Garcia-Granda, S.; Gould, R. O. (2008). The DIRDIF-2008 program system. Crystallography Laboratory, Radboud University Nijmegen, The Netherlands.

^dSheldrick, G. M. *Acta Crystallogr.* **2015**, C71, 3–8.

^e $S = [\sum w(F_o^2 - F_c^2)^2 / (n - p)]^{1/2}$ (n = number of data; p = number of parameters varied; $w = [\sigma^2(F_o^2) + (0.0199P)^2 + 1.0318P]^{-1}$ where $P = [\text{Max}(F_o^2, 0) + 2F_c^2]/3$).

^f $R_1 = \sum ||F_o| - |F_c|| / \sum |F_o|$; $wR_2 = [\sum w(F_o^2 - F_c^2)^2 / \sum w(F_o^4)]^{1/2}$.

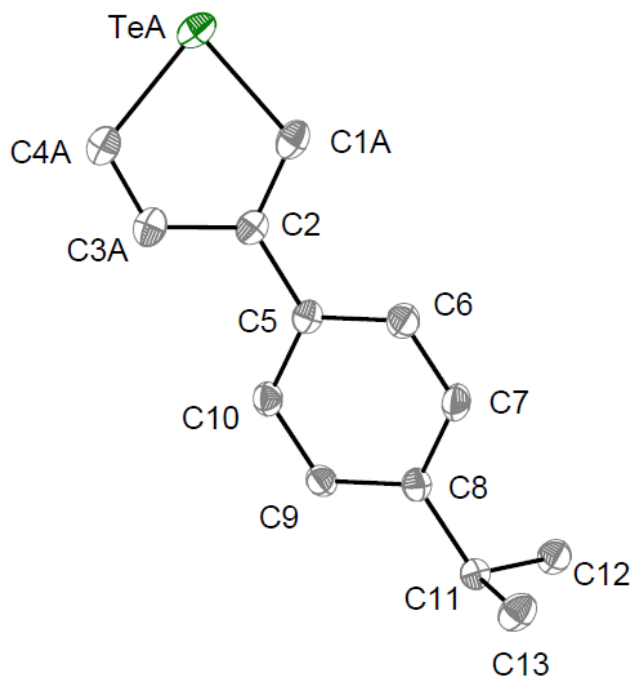


Fig. S6. Molecular structure of 3-(4-isopropylphenyl)-tellurophene (**Te-cumenyl**). Thermal ellipsoids plotted at a 30 % probability level with hydrogen atoms omitted for clarity. Selected bond lengths (Å), angle and dihedral angle (°): Te-C1 2.053(9), Te-C4 2.088(5), C2-C5 1.486(3); C4-Te-C1 80.4(3); C1-C2-C5-C6 24.9(13).

Table S4. Crystallographic experimental details for 3-(4-isopropylphenyl)-tellurophene (**Te-cumenyl**).

A. Crystal Data

| | |
|---|------------------------------------|
| formula | C ₁₃ H ₁₄ Te |
| formula weight | 297.84 |
| crystal dimensions (mm) | 0.41 × 0.18 × 0.04 |
| crystal system | orthorhombic |
| space group | <i>Pbca</i> (No. 61) |
| unit cell parameters ^a | |
| <i>a</i> (Å) | 9.1429 (5) |
| <i>b</i> (Å) | 8.1178 (5) |
| <i>c</i> (Å) | 31.1553 (18) |
| <i>V</i> (Å ³) | 2312.4 (2) |
| <i>Z</i> | 8 |
| ρ_{calcd} (g cm ⁻³) | 1.711 |
| μ (mm ⁻¹) | 2.532 |

Table S4 (con't):**B. Data Collection and Refinement Conditions**

| | |
|--|--|
| diffractometer | Bruker D8/APEX II CCD ^b |
| radiation (λ [Å]) | graphite-monochromated Mo K α (0.71073) |
| temperature (°C) | –100 |
| scan type | ω scans (0.3°) (15 s exposures) |
| data collection 2θ limit (deg) | 55.05 |
| total data collected | 19073 ($-11 \leq h \leq 11$, $-10 \leq k \leq 10$, $-40 \leq l \leq 38$) |
| independent reflections | 2658 ($R_{\text{int}} = 0.0381$) |
| number of observed reflections (<i>NO</i>) | 2173 [$F_o^2 \geq 2\sigma(F_o^2)$] |
| structure solution method | Patterson/structure expansion (<i>DIRDIF-2008</i> ^c) |
| refinement method | full-matrix least-squares on F^2 (<i>SHELXL-2014</i> ^d) |
| absorption correction method | Gaussian integration (face-indexed) |
| range of transmission factors | 0.9485–0.5244 |
| data/restraints/parameters | 2658 / 5 ^e / 149 |
| goodness-of-fit (<i>S</i>) ^f [all data] | 1.059 |
| final <i>R</i> indices ^g | |
| R_1 [$F_o^2 \geq 2\sigma(F_o^2)$] | 0.0319 |
| wR_2 [all data] | 0.0840 |
| largest difference peak and hole | 0.573 and –0.466 e Å ^{–3} |

^aObtained from least-squares refinement of 6265 reflections with $5.24^\circ < 2\theta < 45.62^\circ$.

^bPrograms for diffractometer operation, data collection, data reduction and absorption correction were those supplied by Bruker.

^cBeurskens, P. T.; Beurskens, G.; de Gelder, R.; Smits, J. M. M.; Garcia-Granda, S.; Gould, R. O. (2008). The *DIRDIF-2008* program system. Crystallography Laboratory, Radboud University Nijmegen, The Netherlands.

^dSheldrick, G. M. *Acta Crystallogr.* **2015**, *C71*, 3–8.

^eThe following pairs of distances within the disordered tellurophene group were constrained to be equal (within 0.03 Å) during refinement: d(TeA–C1A) = d(TeB–C1B); d(TeA–C4A) = d(TeB–C4B); d(C1A–C2) = d(C1B–C2); d(C2–C3A) = d(C2–C3B); d(C3A–C4A) = d(C3B–C4B).

^f $S = [\sum w(F_o^2 - F_c^2)^2 / (n - p)]^{1/2}$ (n = number of data; p = number of parameters varied; $w = [\sigma^2(F_o^2) + (0.0382P)^2 + 1.7401P]^{-1}$ where $P = [\text{Max}(F_o^2, 0) + 2F_c^2]/3$).

^g $R_1 = \sum ||F_o| - |F_c|| / \sum |F_o|$; $wR_2 = [\sum w(F_o^2 - F_c^2)^2 / \sum w(F_o^4)]^{1/2}$.

5. NMR Spectroscopy

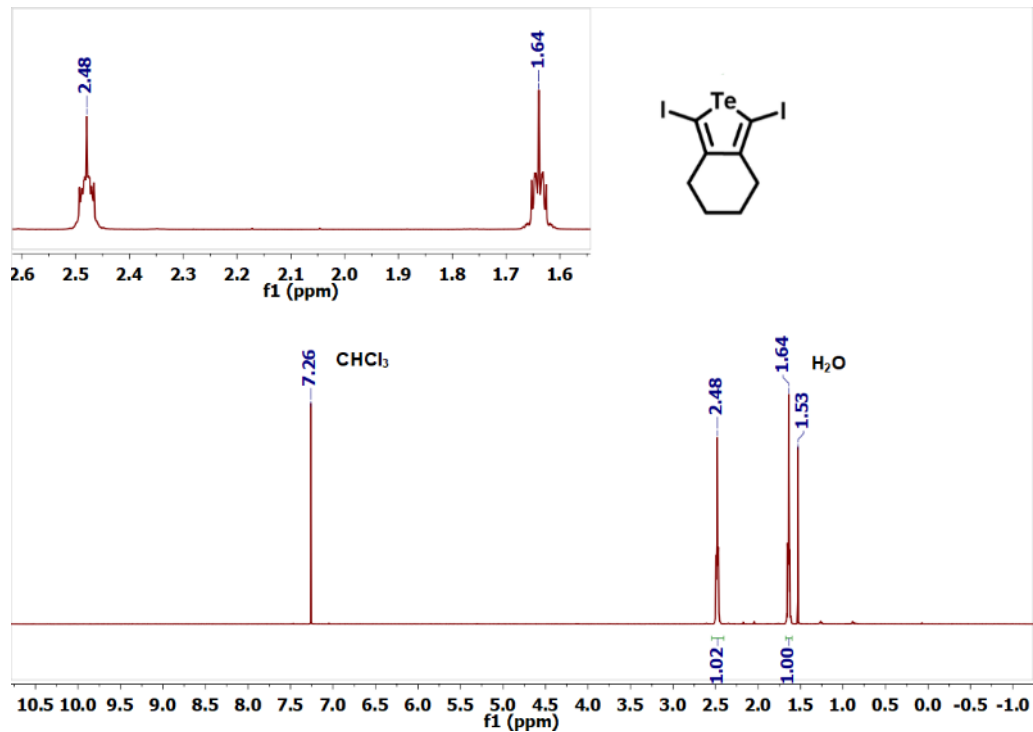


Fig. S7. ^1H NMR spectrum (500 MHz) of 1,3-diiodo-4,5,6,7-tetrahydro-benzo[*c*]tellurophene (I-Te-6-I) in CDCl_3 .

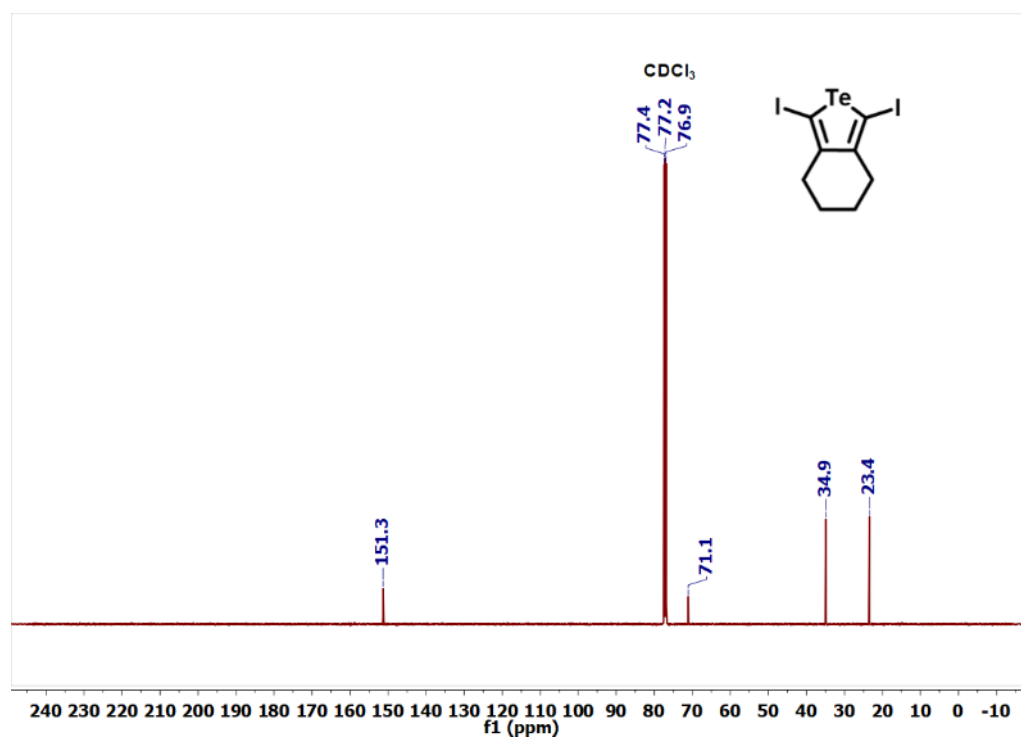


Fig. S8. $^{13}\text{C}\{^1\text{H}\}$ NMR spectrum (126 MHz) of 1,3-diiodo-4,5,6,7-tetrahydro-benzo[*c*]tellurophene (I-Te-6-I) in CDCl_3 .

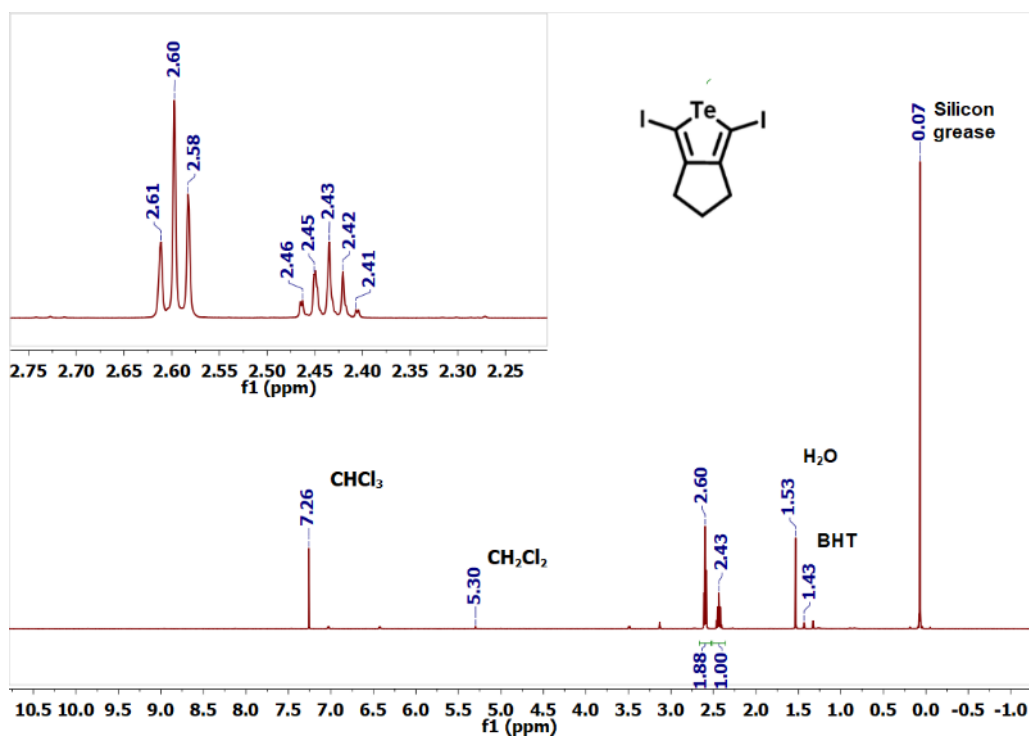


Fig. S9. ^1H NMR spectrum (500 MHz) of 1,3-diiodo-4,5,6,7-tetrahydro-cyclopenta[c]-tellurophene (**I-Te-5-I**) in CDCl_3 ; BHT = trace butylated hydroxytoluene.

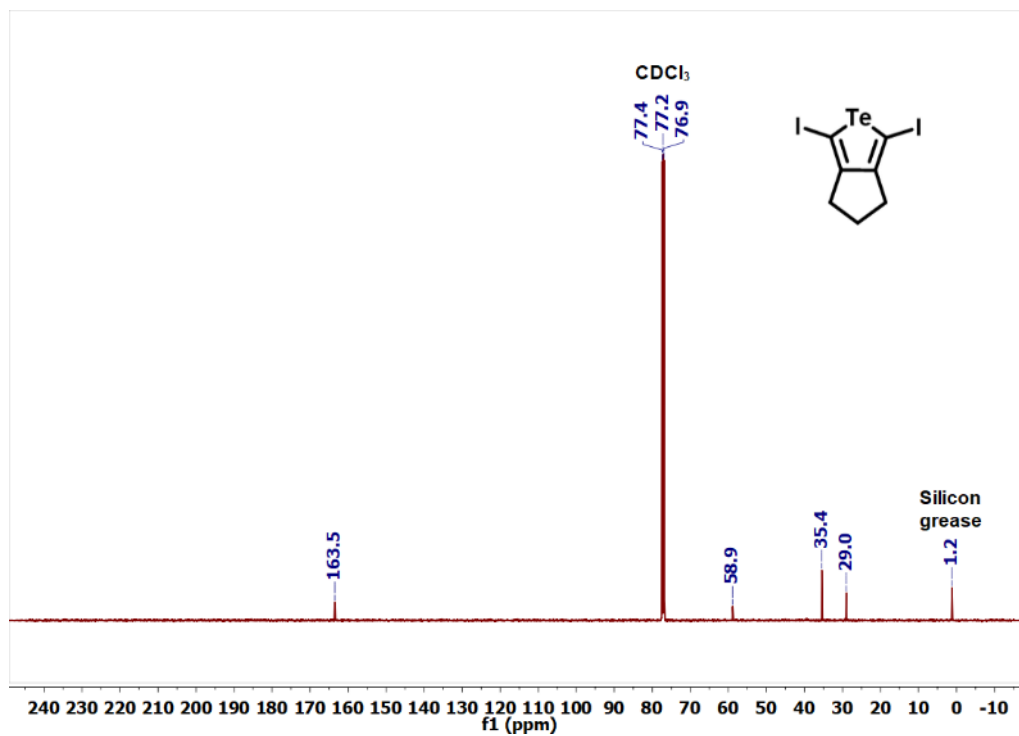


Fig. S10. $^{13}\text{C}\{^1\text{H}\}$ NMR spectrum (126 MHz) of 1,3-diiodo-4,5,6,7-tetrahydro-cyclopenta[c]-tellurophene (**I-Te-5-I**) in CDCl_3 .

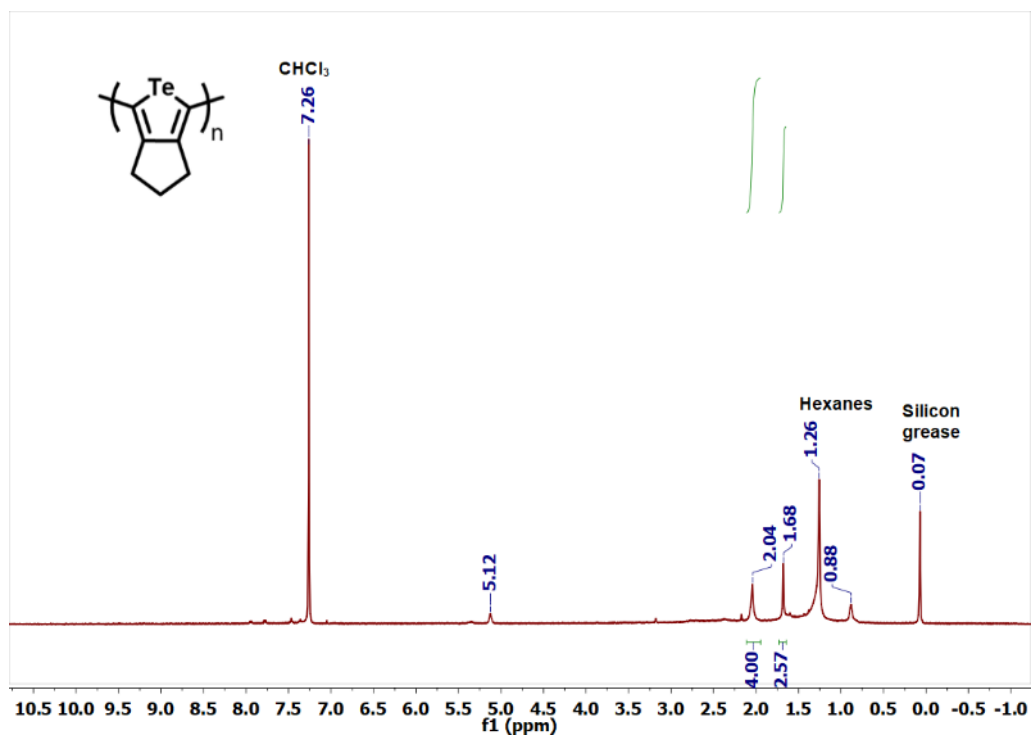


Fig. S11. ¹H NMR spectrum (500 MHz) of **Oligo-Te5** in CDCl₃.

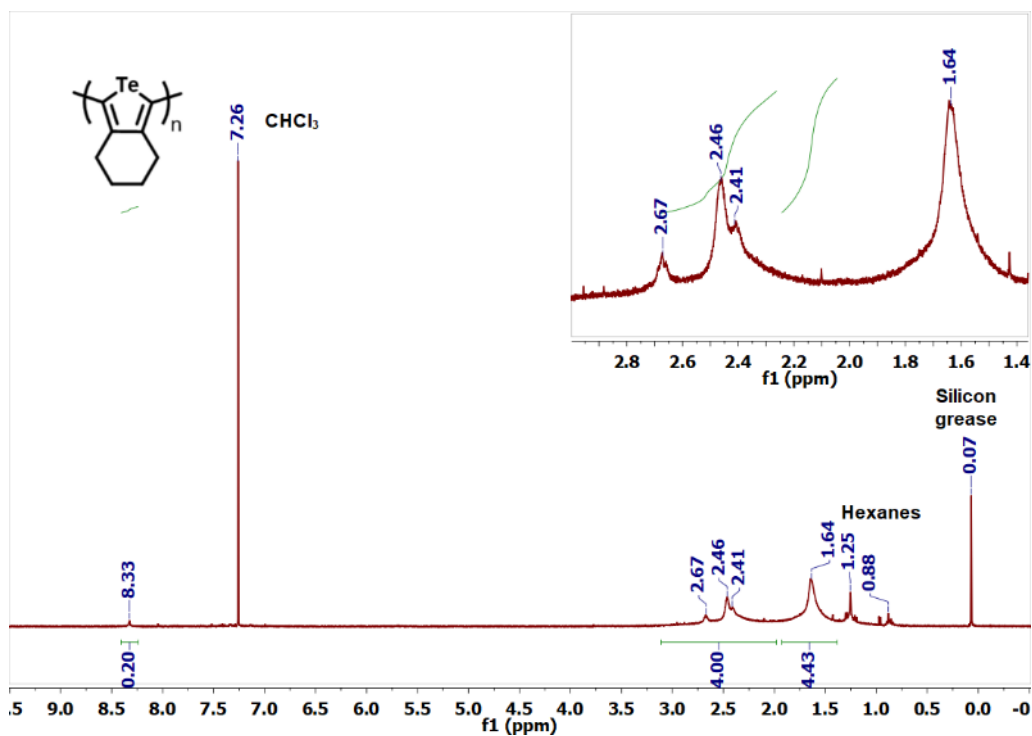


Fig. S12. ¹H NMR spectrum (400 MHz) of **Oligo-Te6** in CDCl₃.

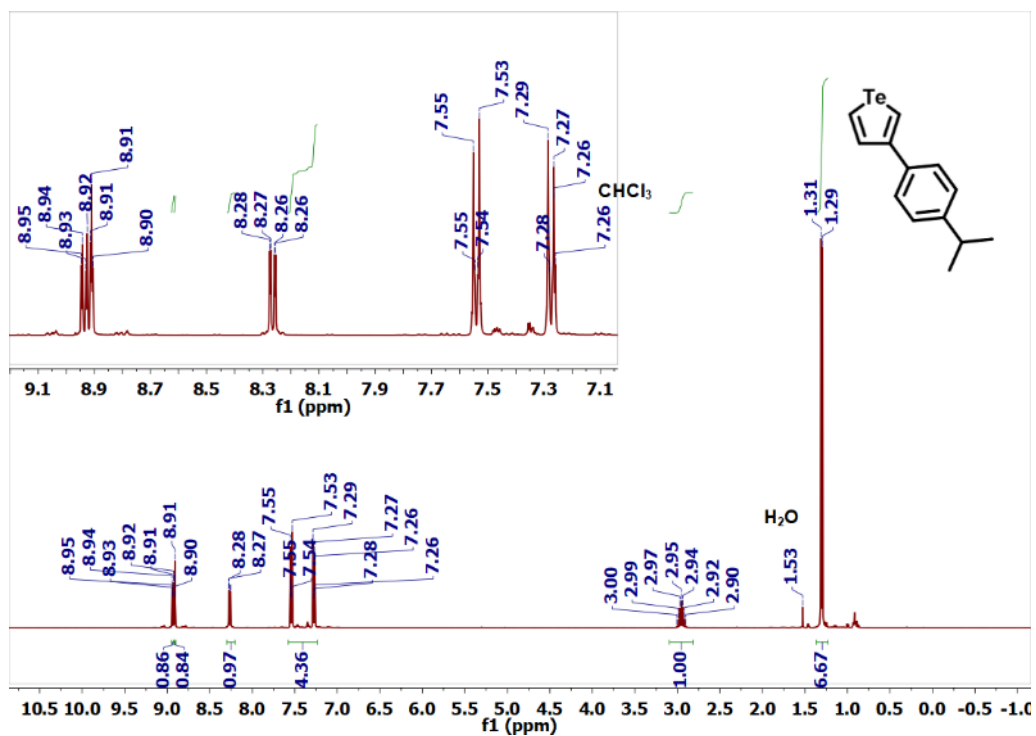


Fig. S13. ¹H NMR spectrum (400 MHz) of 3-(4-isopropylphenyl)-tellurophene (Te-cumenyl) in CDCl₃.

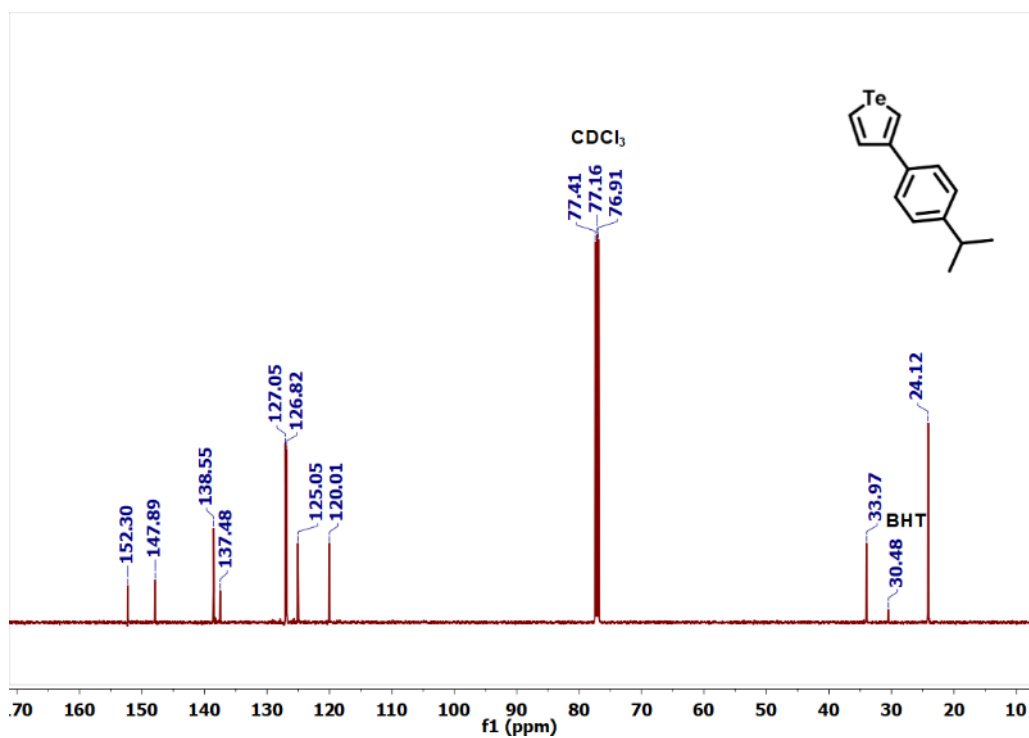


Fig. S14. ¹³C NMR (126 MHz) of 3-(4-isopropylphenyl)-tellurophene (Te-cumenyl) in CDCl₃. BHT = butylated hydroxytoluene.

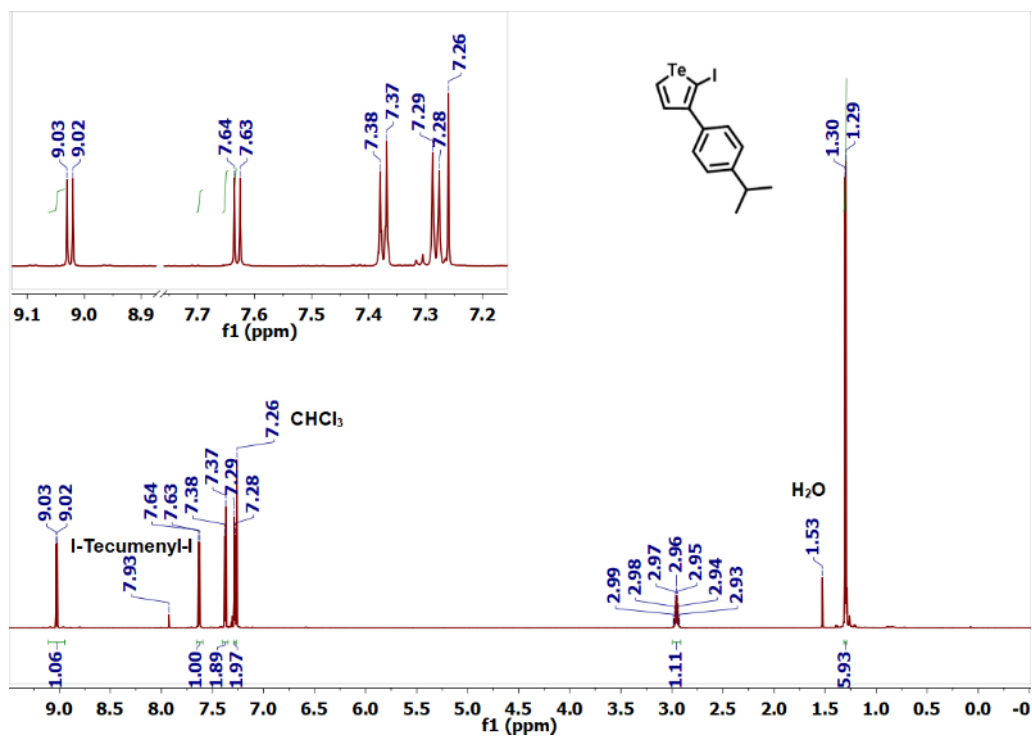


Fig. S15. ^1H NMR spectrum (700 MHz) of crude 2-iodo-3-(4-isopropylphenyl)-tellurophene (H-Te-cumenyl-I) in CDCl_3 .

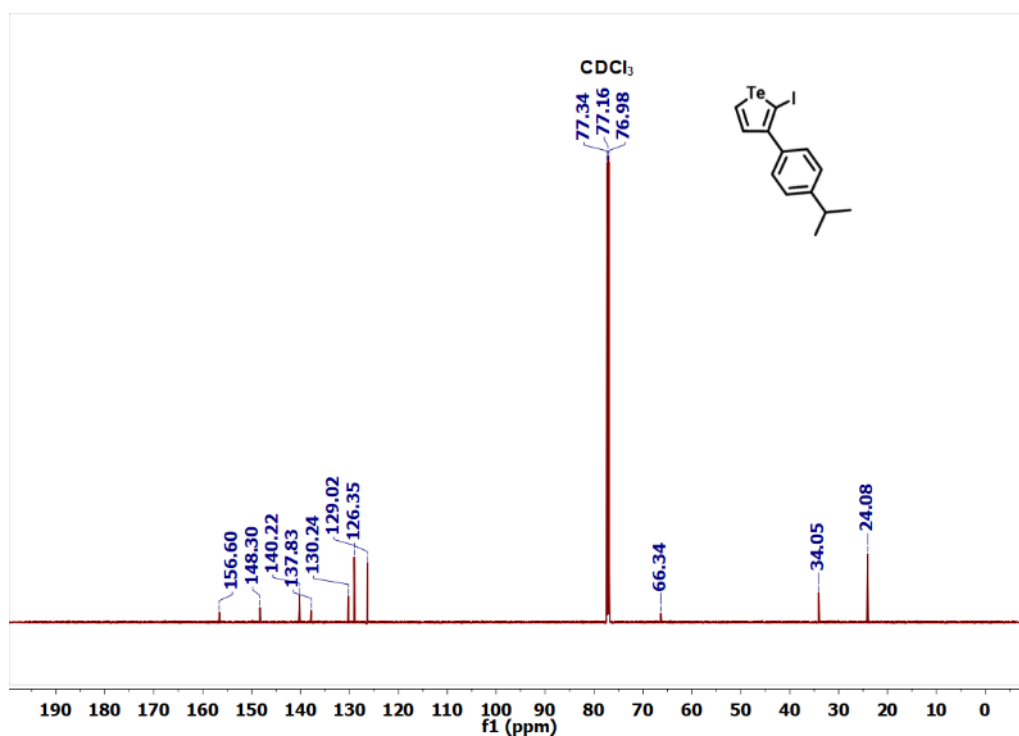


Fig. S16. $^{13}\text{C}\{^1\text{H}\}$ NMR spectrum (176 MHz) of crude 2-iodo-3-(4-isopropylphenyl)-tellurophene (H-Te-cumenyl-I) in CDCl_3 .

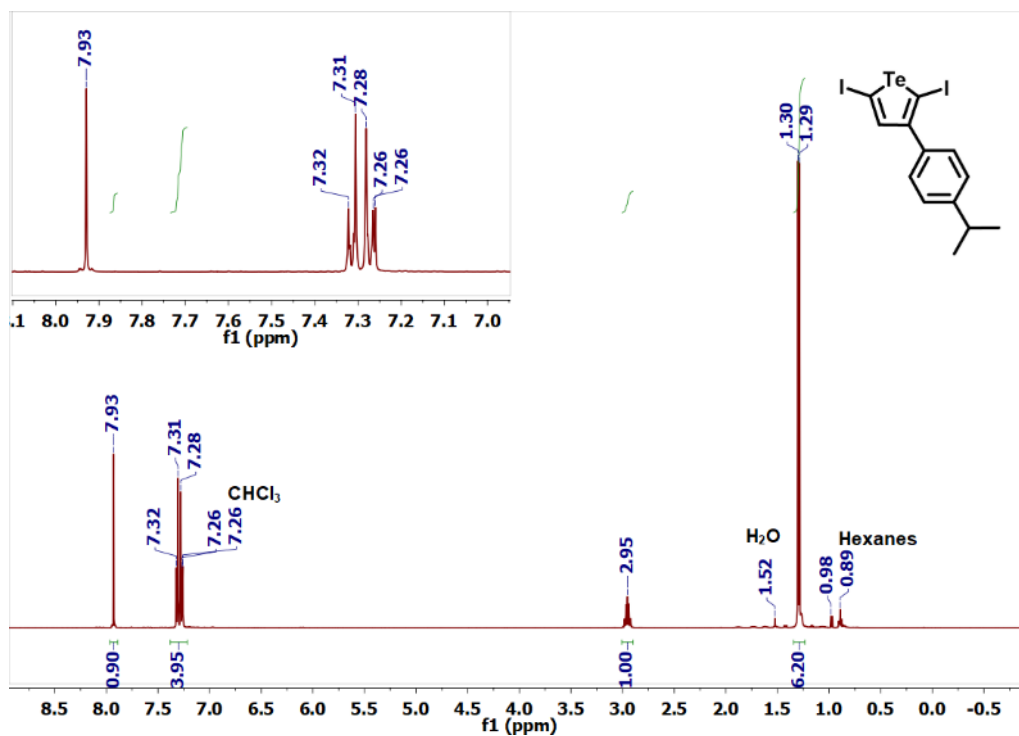


Fig. S17. ^1H NMR spectrum (500 MHz) of 2,5-diiodo-3-(4-isopropylphenyl)-tellurophene (I-Te-cumenyl-I) in CDCl_3 .

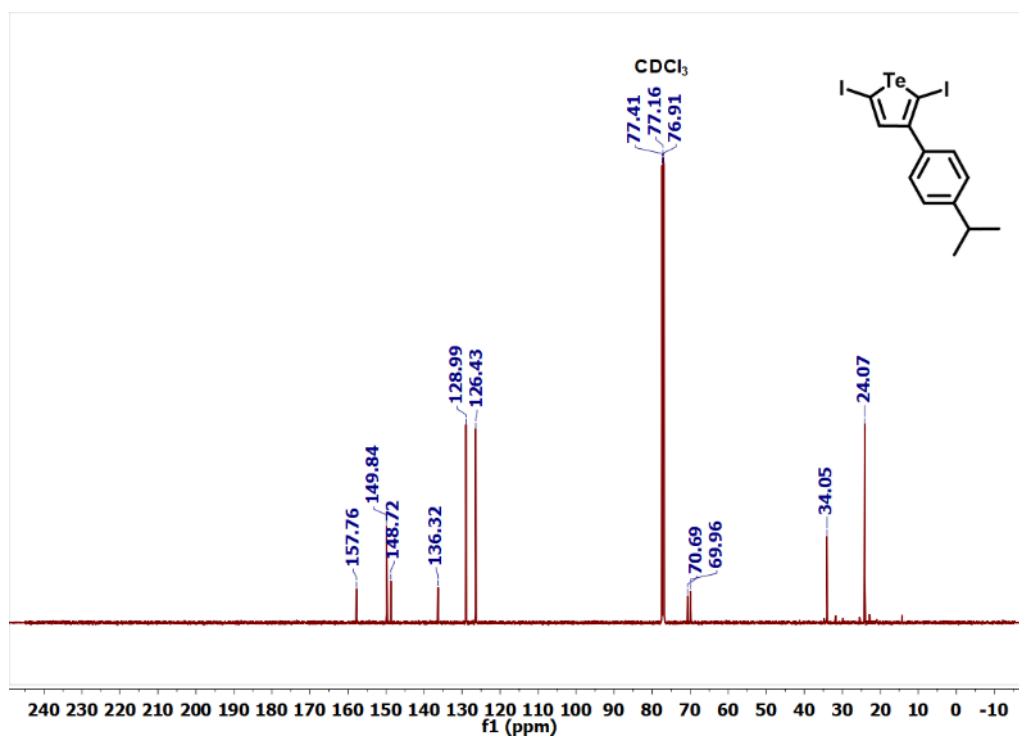


Fig. S18. $^{13}\text{C}\{^1\text{H}\}$ NMR spectrum (126 MHz) of 2,5-diiodo-3-(4-isopropylphenyl)-tellurophene (I-Te-cumenyl-I) in CDCl_3 .

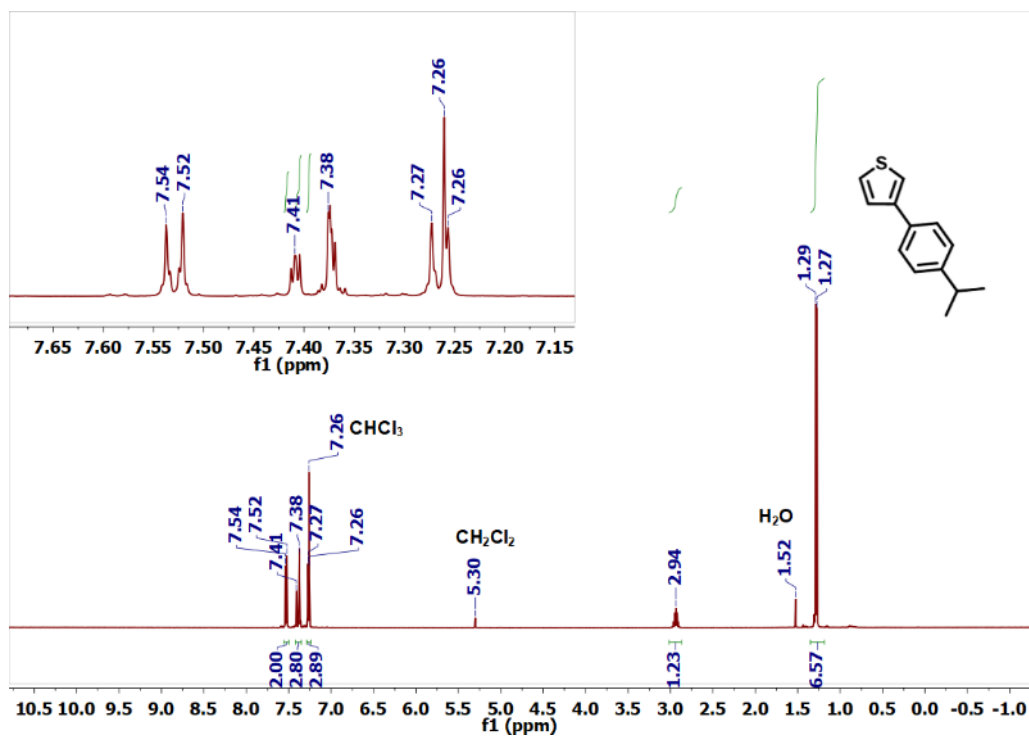


Fig. S19. ^1H NMR spectrum (500 MHz) of 3-(4-isopropylphenyl)-thiophene (**S-cumenyl**) in CDCl_3 .

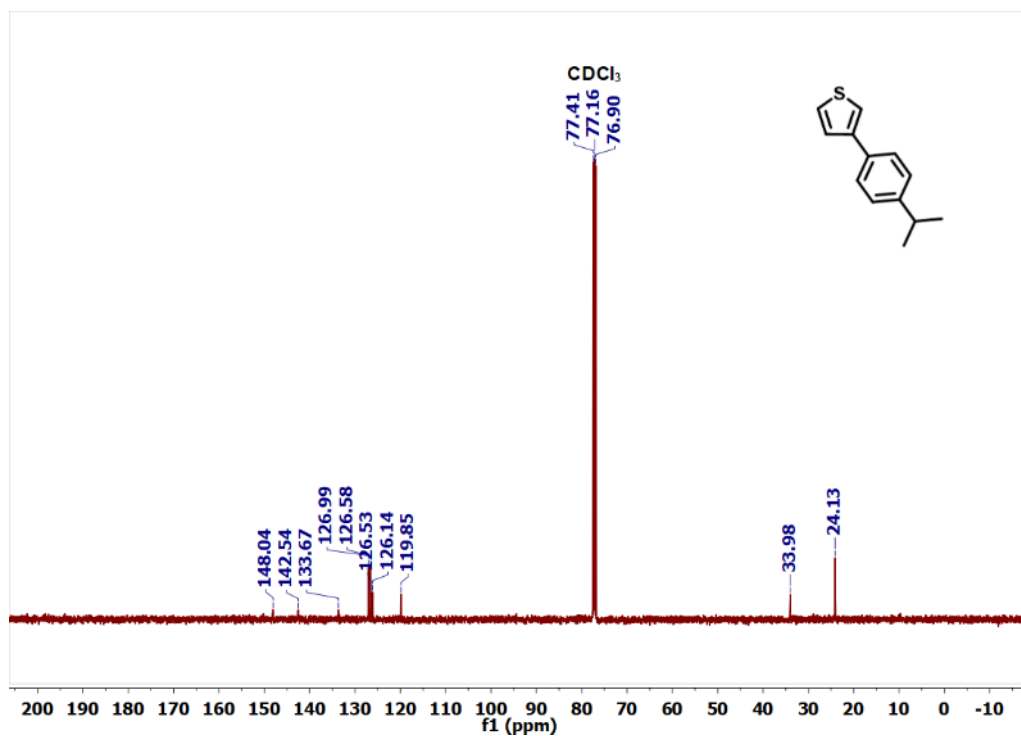


Fig. S20. $^{13}\text{C}\{^1\text{H}\}$ NMR spectrum (126 MHz) of 3-(4-isopropylphenyl)-thiophene (**S-cumenyl**) in CDCl_3 .

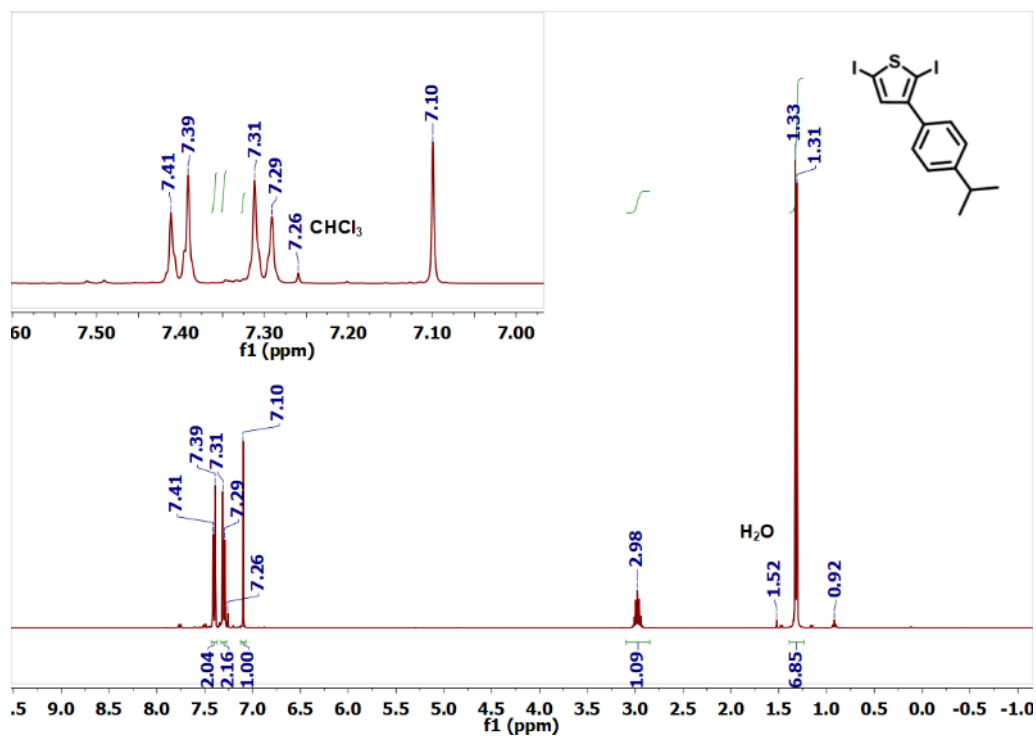


Fig. S21. ¹H NMR spectrum (400 MHz) of 2,5-diiodo-3-(4-isopropylphenyl)-thiophene (*I-S-cumenyl-I*) in CDCl₃.

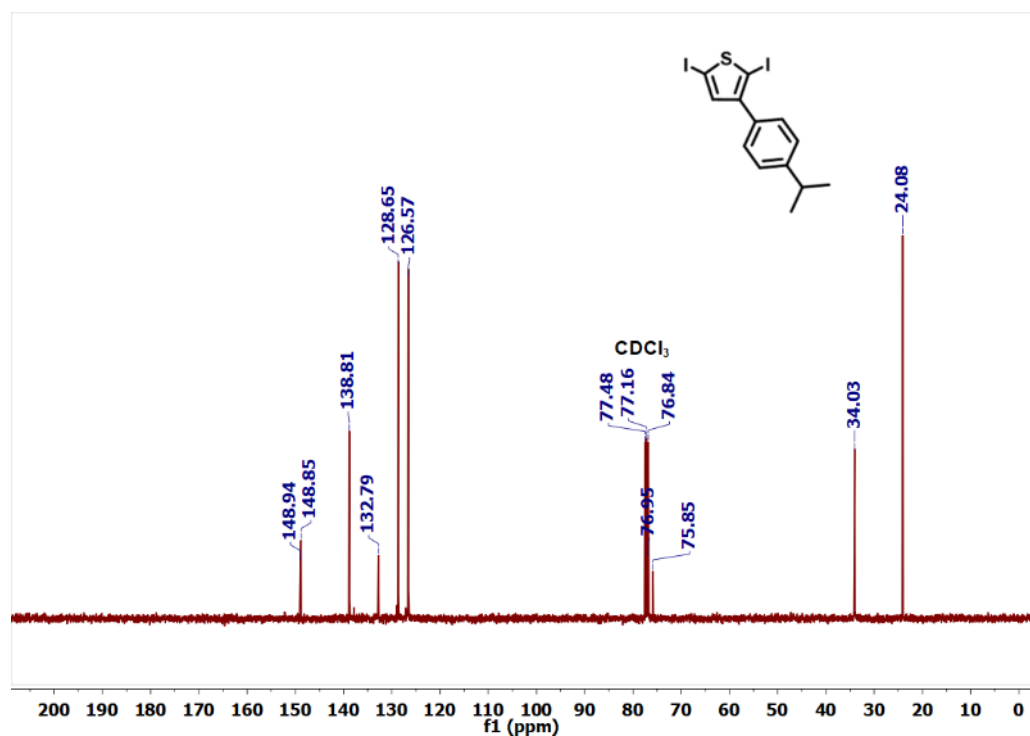


Fig. S22. ¹³C{¹H} NMR spectrum (101 MHz) of 2,5-diiodo-3-(4-isopropylphenyl)-thiophene (*I-S-cumenyl-I*) in CDCl₃.

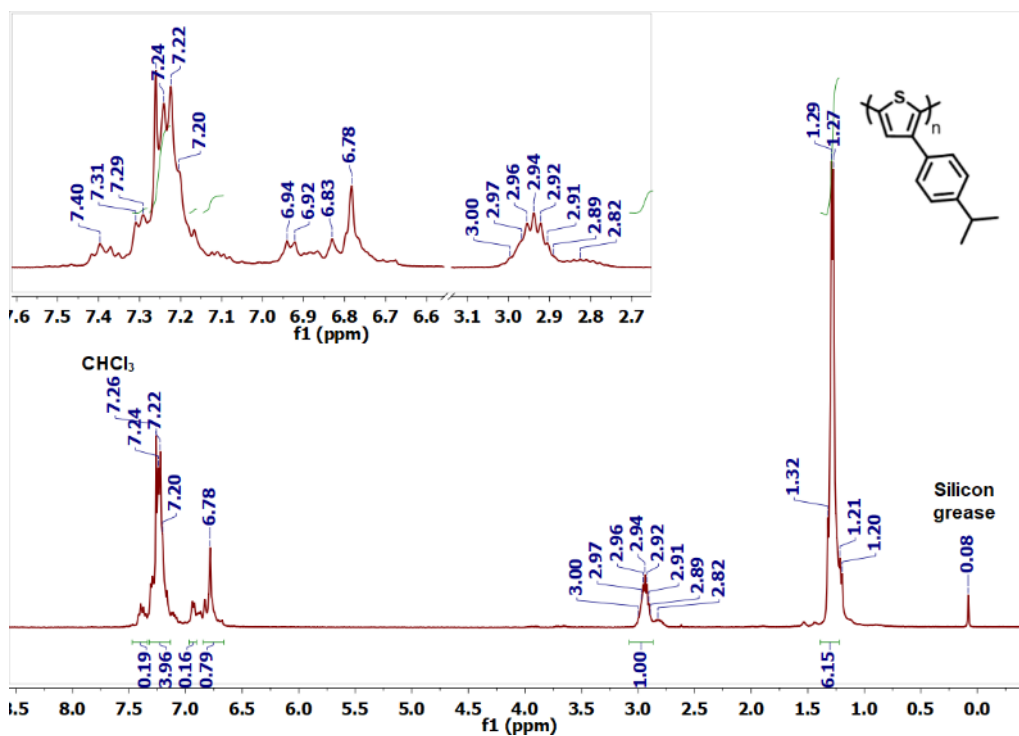


Fig. S23. ^1H NMR spectrum (400 MHz) of poly(3-(4-isopropylphenyl)-thiophene) (PolyS-cumenyl) in CDCl_3 .

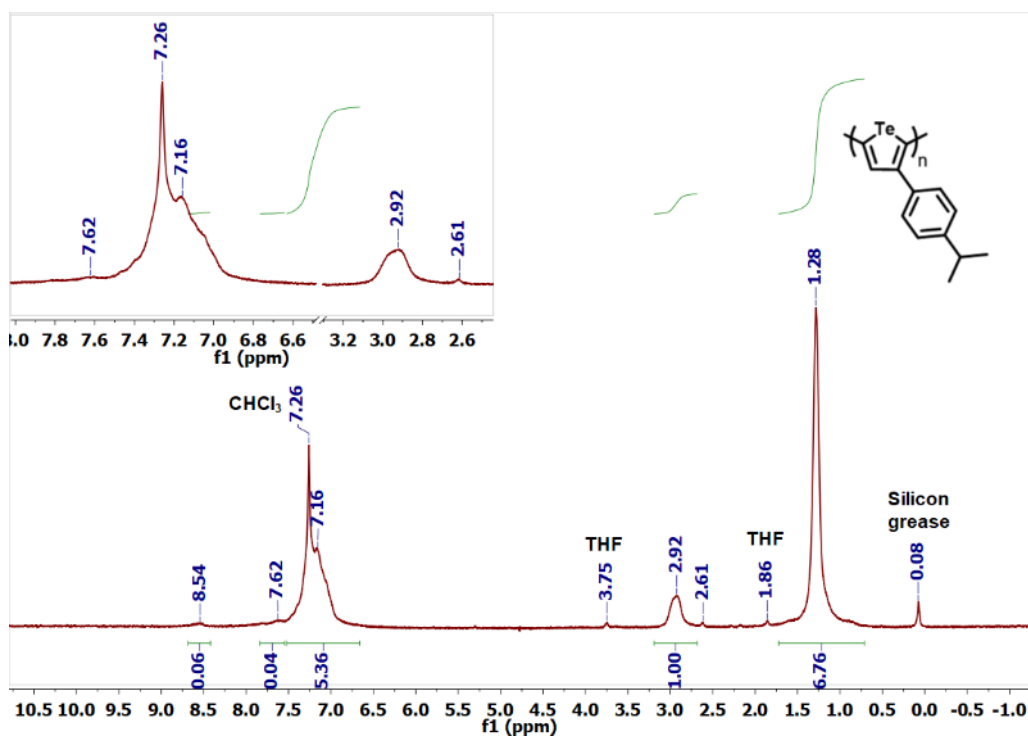


Fig. S24. ^1H NMR spectrum (500 MHz) of poly(3-(4-isopropylphenyl)-tellurophene) (PolyTe-cumenyl) in CDCl_3 .

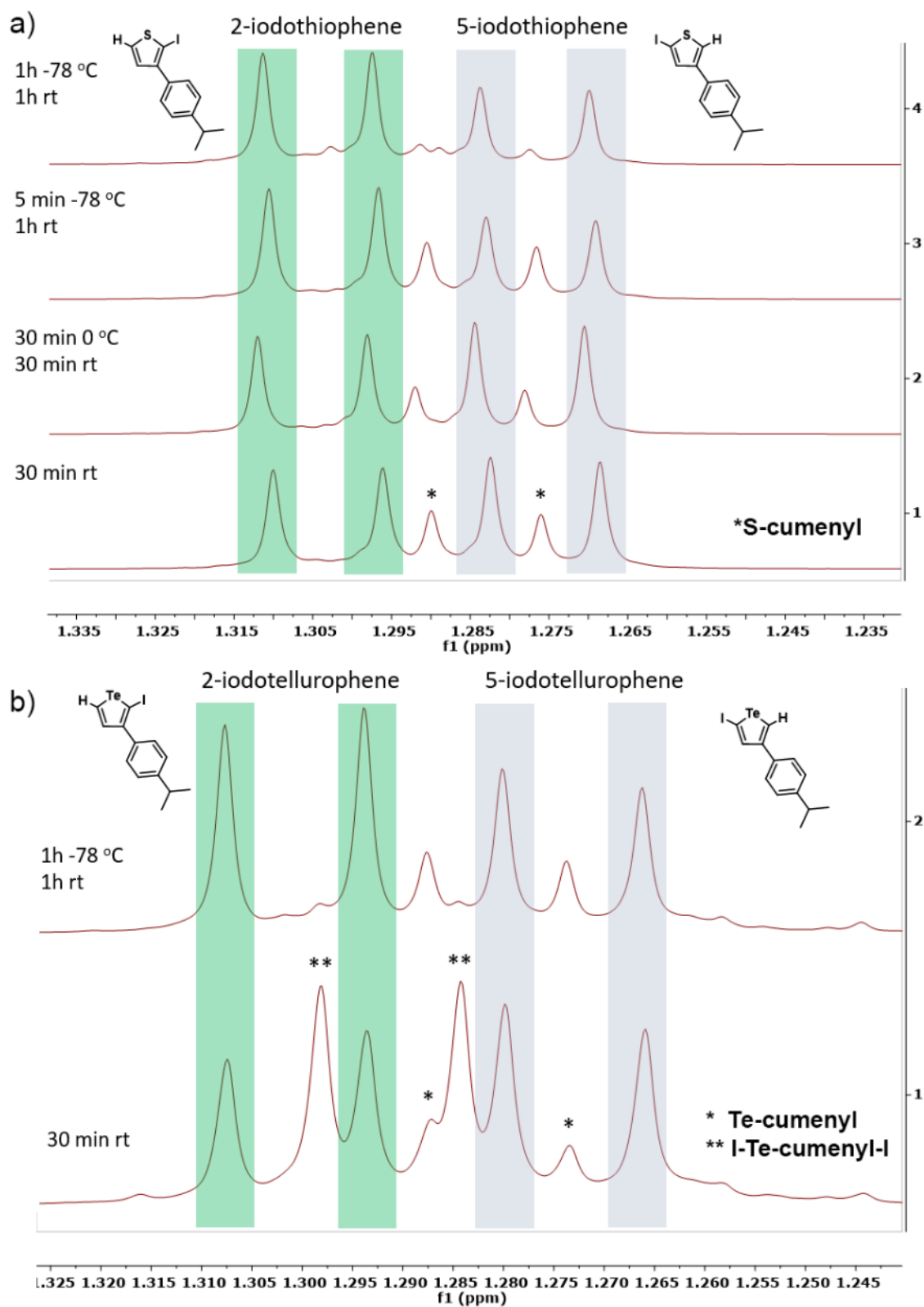


Fig. S25. ^1H NMR study of GRIM activation step for **I-S-cumenyl-I** (a) and **I-Te-cumenyl-I** (b) with $^i\text{PrMgCl}\cdot\text{LiCl}$ at different temperatures after quenching the reaction mixture with dilute HCl. In both cases, double-metallation of the monomer is observed even at $-78\text{ }^\circ\text{C}$.

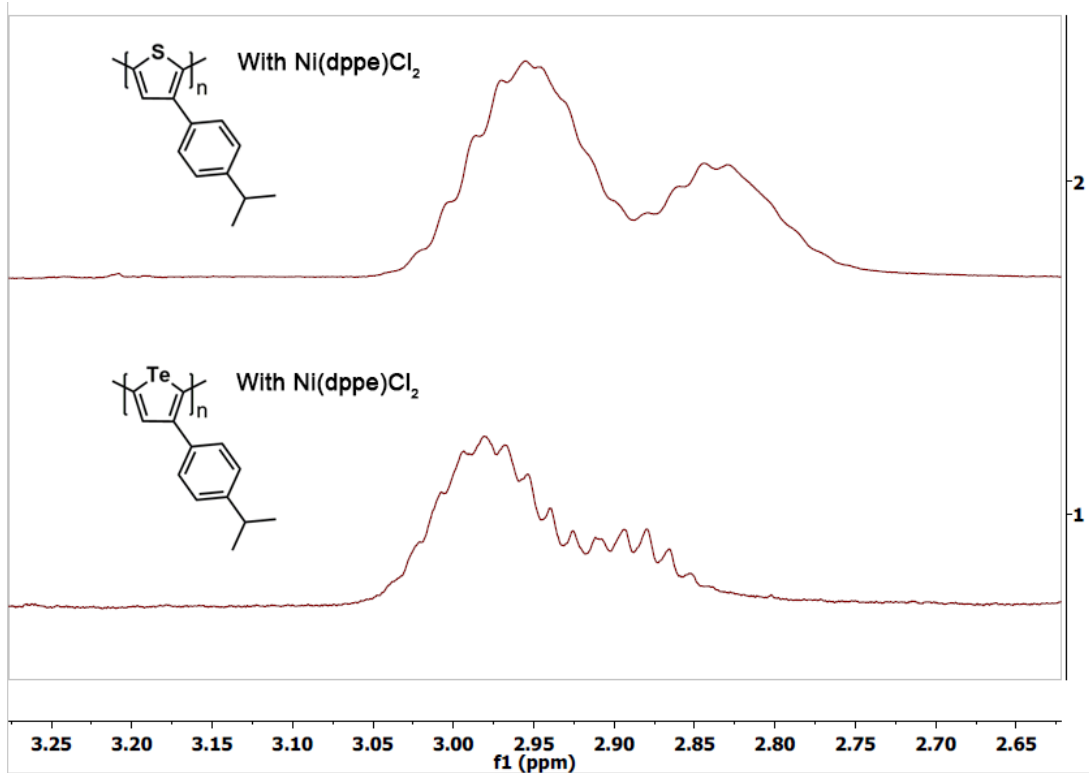


Fig. S26. ^1H NMR of the isopropyl region of polymers with low regioregularity obtained during polymerization trials with $\text{Ni}(\text{dppe})\text{Cl}_2$ (1 mol%). **PolyS-cumenyl** ($M_w = 13$ kDa, PDI = 1.1; 65 % regioregularity) was synthesized at 80 °C and recovered in the hexanes fraction via Soxhlet. **PolyTe-cumenyl** ($M_w = 4.1$ kDa, PDI = 1.5; 73 % regioregularity) was synthesized at 40 °C and recovered in the CHCl_3 Soxhlet fraction.

6. UV-Vis spectroscopy

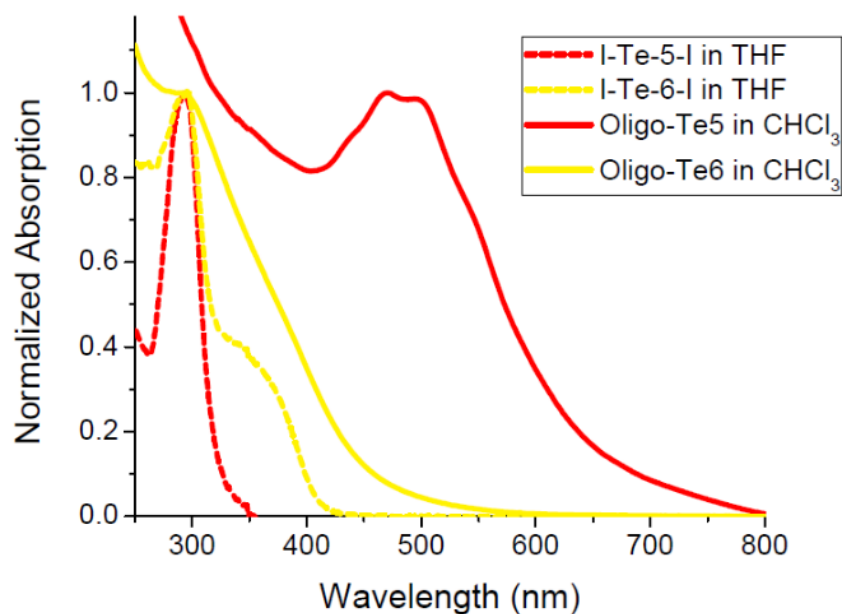


Fig. S27. UV-Vis spectra of **I-Te-5-I** and **I-Te-6-I** in THF and respective oligomer mixtures **Oligo-Te5** and **Oligo-Te6** in CHCl₃. Estimated onset of absorption for oligomer solutions: **Oligo-Te6**: 456 nm; **Oligo-Te5**: 629 nm.

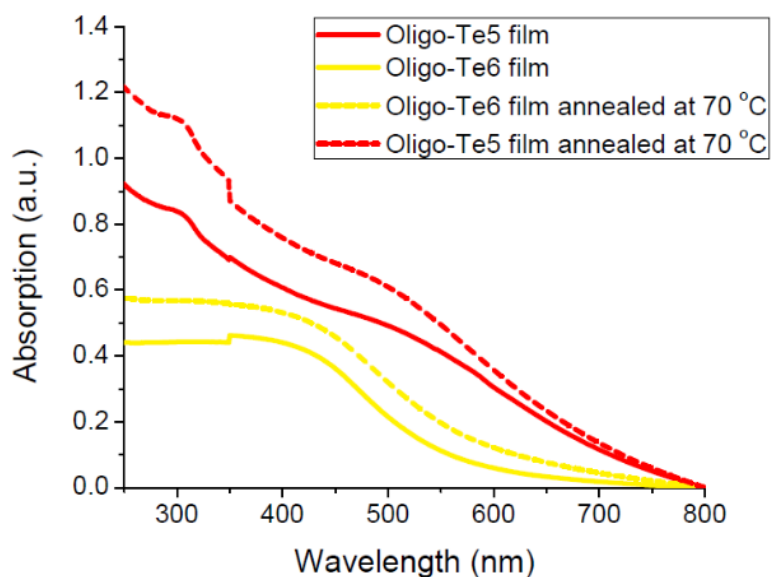


Fig. S28. UV-Vis spectra of **Oligo-Te6** and **Oligo-Te5** (as drop-cast films from CHCl₃) before and after annealing at 70 °C. Estimated onset of absorption: **Oligo-Te6**: 558 nm; **Oligo-Te5**: 683 nm.

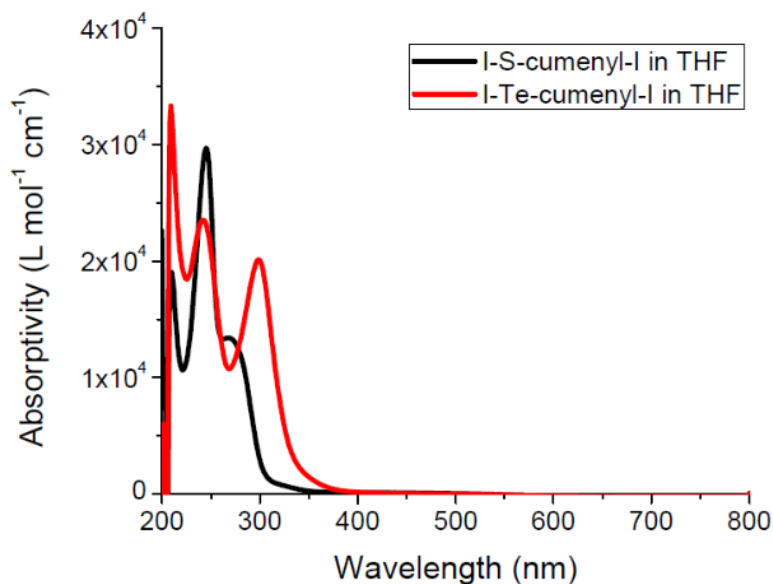


Fig. S29. UV-Vis spectra of **I-S-cumenyl-I** and **I-Te-cumenyl-I** in THF.

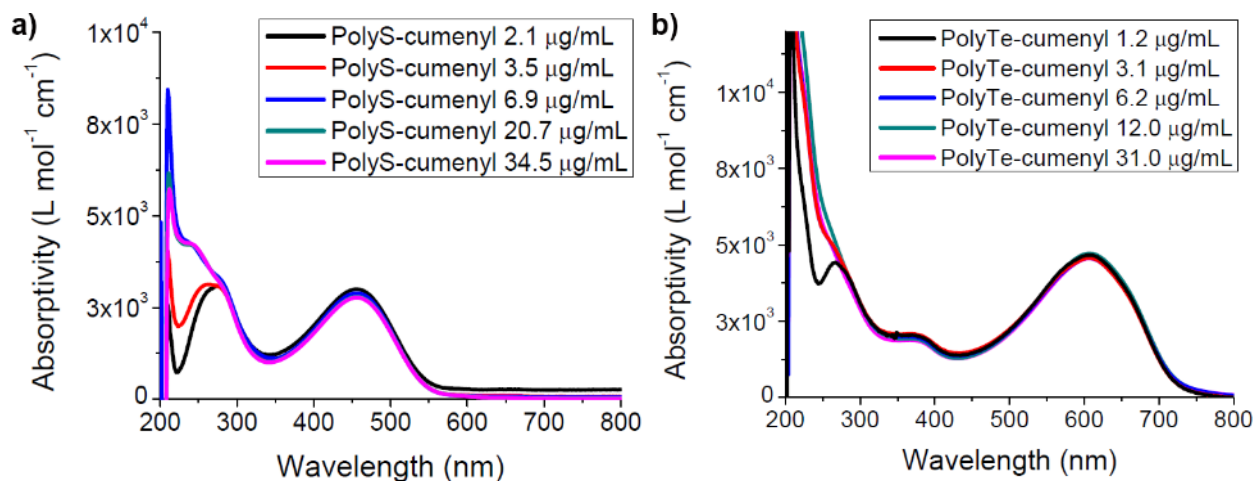


Fig. S30. UV-Vis spectra of **PolyS-cumenyl** (a) and **PolyTe-cumenyl** (b) in THF solutions at different concentrations. A shoulder appears at ~ 250 nm as the concentration increases, indicating some degree of intermolecular interaction. Estimated onset of absorption: **PolyS-cumenyl**: 544 nm; **PolyTe-cumenyl**: 721 nm.

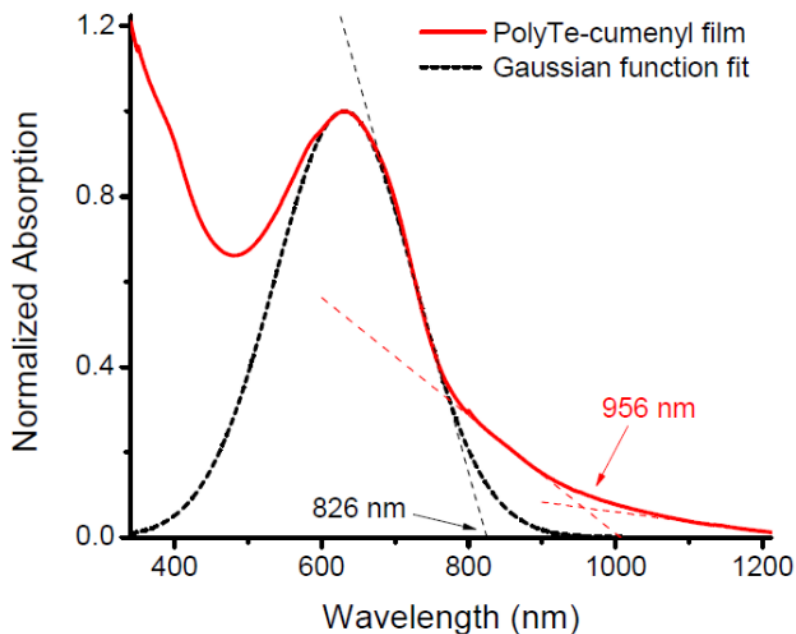


Fig. S31. Determination of the onset of absorption for a film of **PolyTe-cumenyl**. The intersection of linear fits (red dashed lines) at the initial absorption increase (<1000 nm) and at long wavelengths (>1100 nm) was used to determine the optical HOMO/LUMO gap (956 nm; $E_g = 1.30$ eV). To account for the possibility of light scattering effects at long wavelengths, a more conservative onset was determined by fitting a Gaussian function to the main peak and determining the intersection of a linear fit (black dashed line) with the wavelength axis (826 nm; $E_g = 1.50$ eV). The Gaussian function is centered at 631 nm and has root mean square width of 95 nm.

7. MALDI Mass Spectrometry

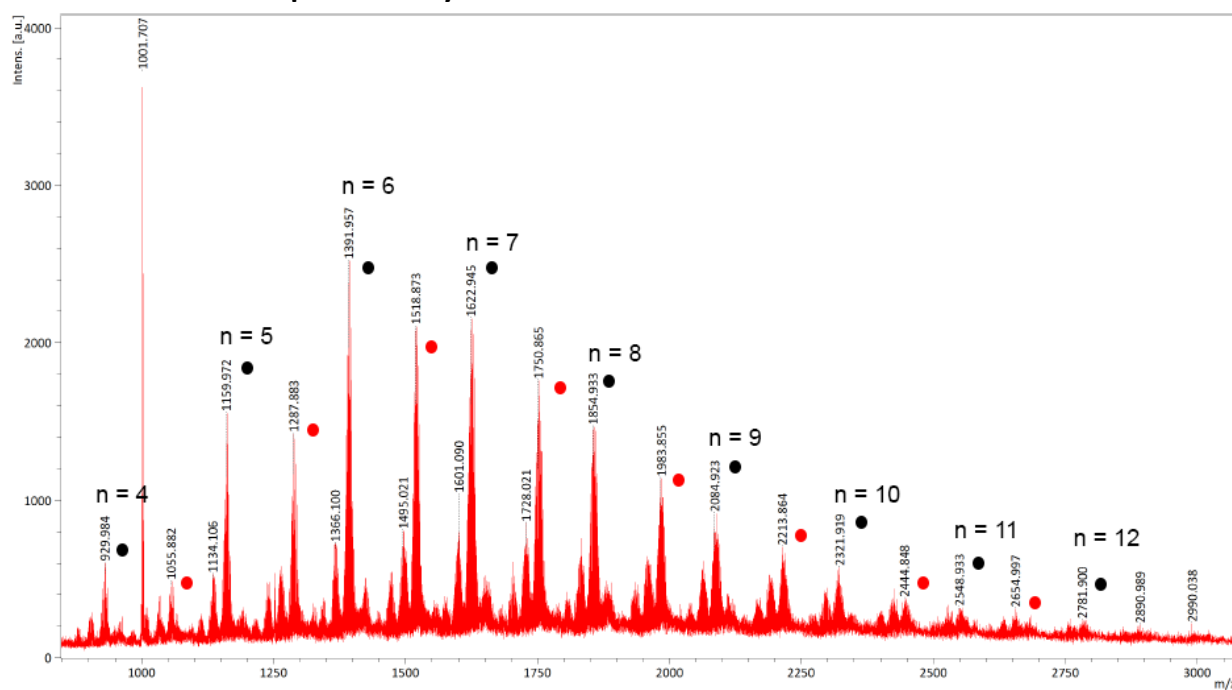


Fig. S32. MALDI-MS of **Oligo-Te6**. Black dots represent H/H termination, red dots represent H/I termination.

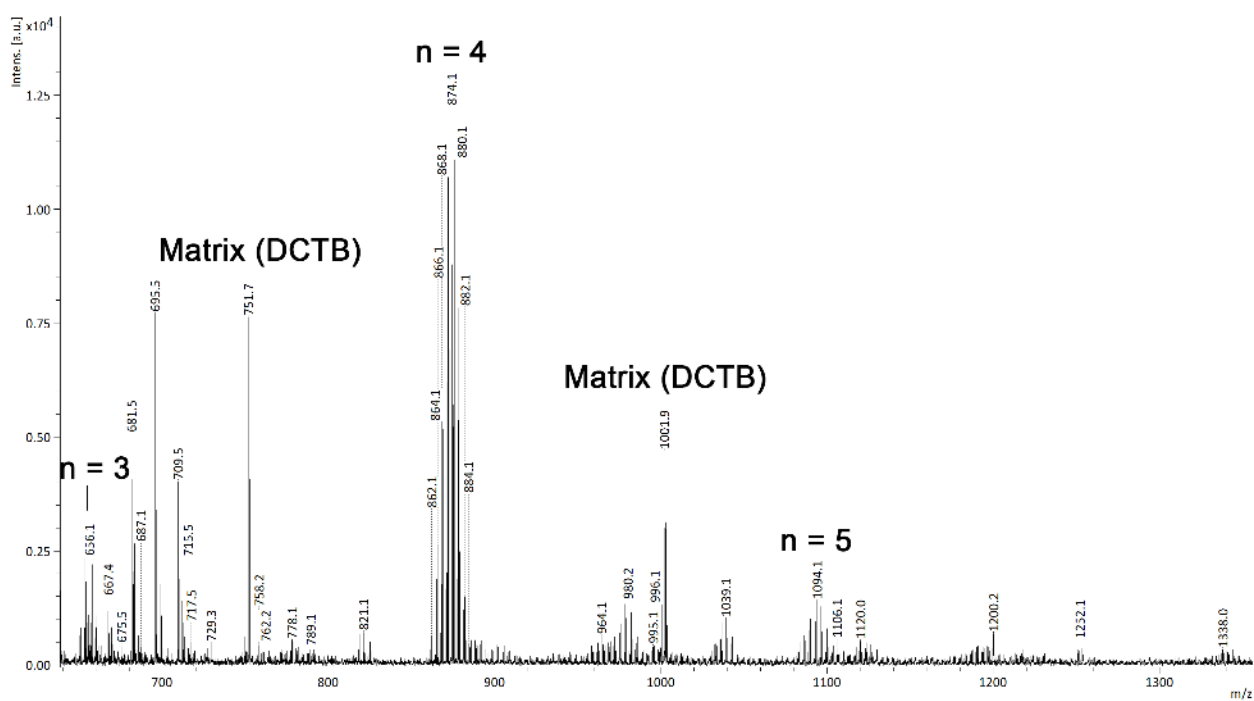


Fig. S33. MALDI-MS of **Oligo-Te5**. The marked peaks correspond to oligomers showing mass matching H/H termination.

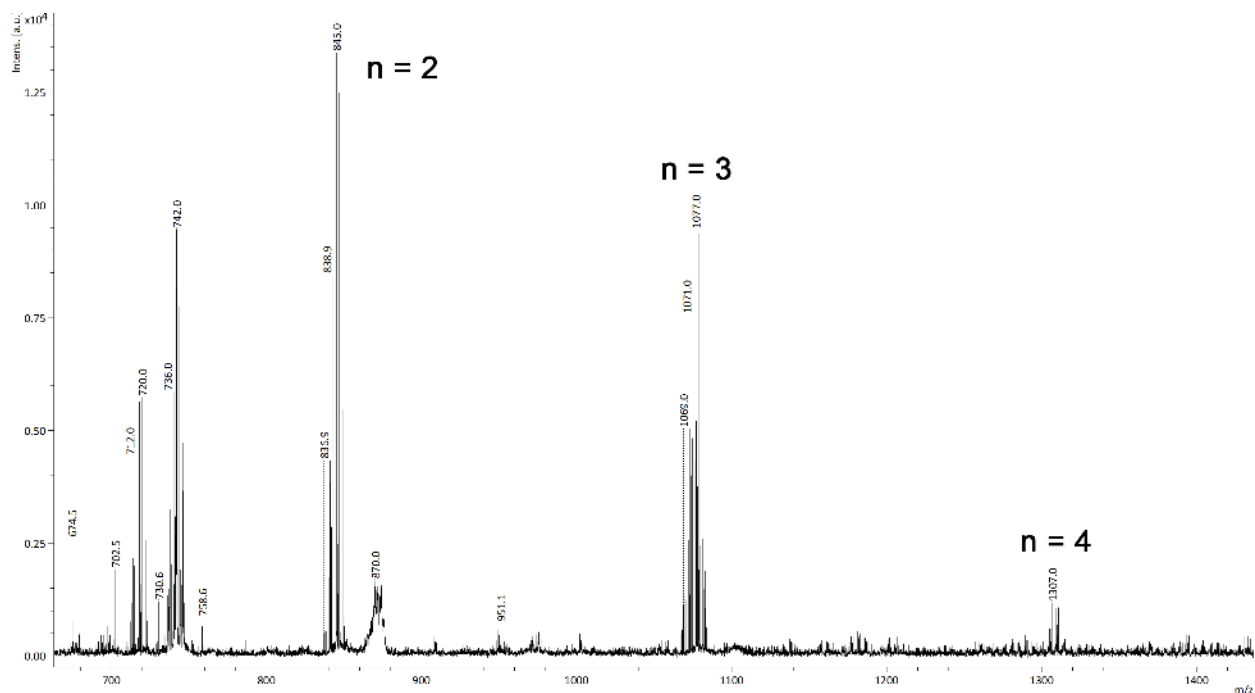


Fig. S34. MALDI-MS of a self-oligomerized sample of **I-Te-6-I**. Isotope pattern of the oligomers suggest that additional doping (oxidation) by I_2 occurred to yield three iodine atoms per oligomer.

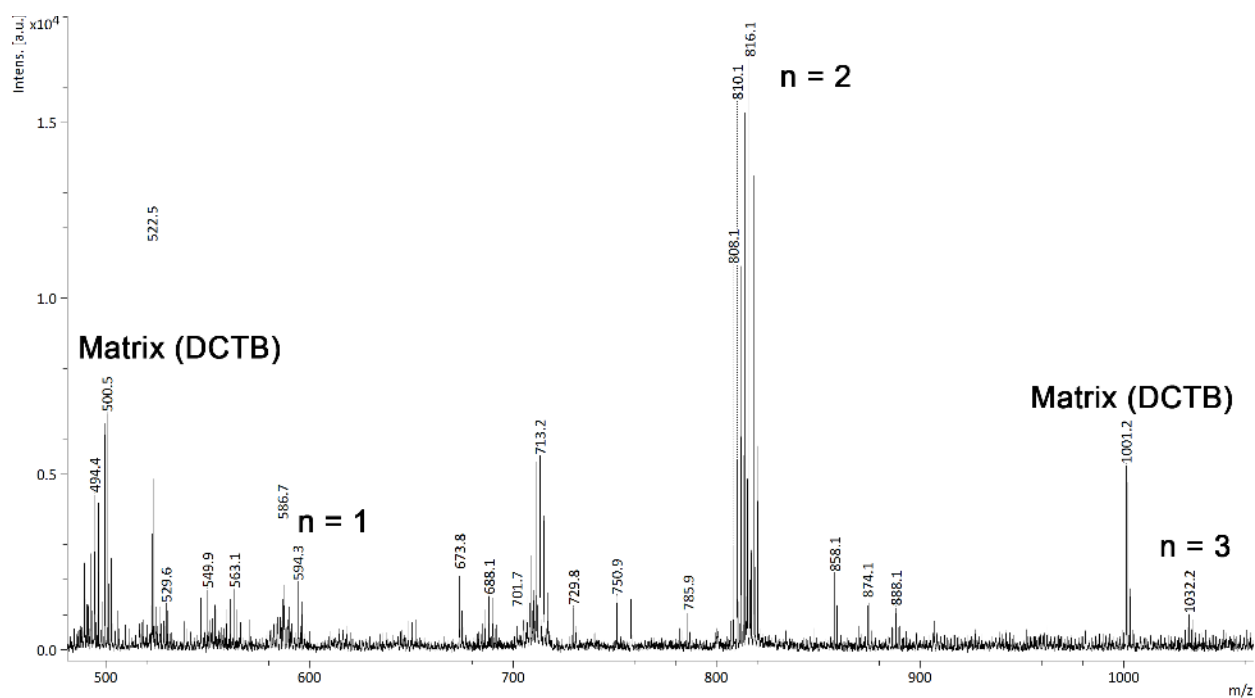


Fig. S35. MALDI-MS of a self-oligomerized sample of **I-Te-5-I**. Isotope pattern of the oligomers suggest that additional doping (oxidation) by I_2 occurred to yield three iodine atoms per oligomer.

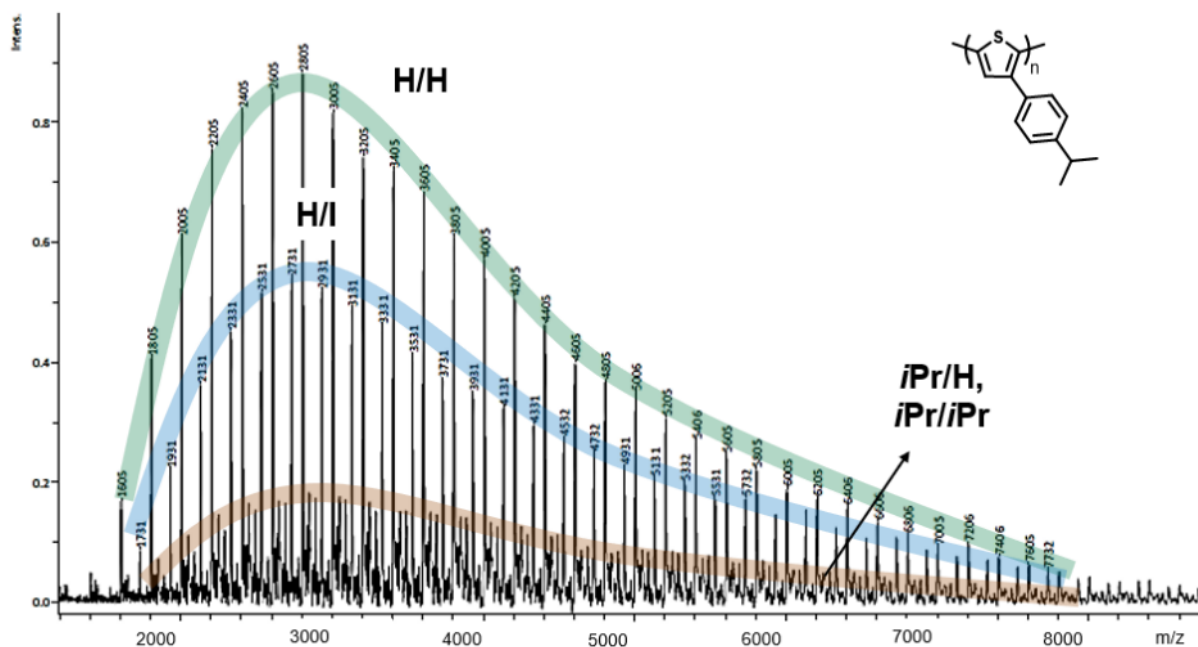


Fig. S36. MALDI-MS of PolyS-cumenyl. Green curve highlights H/H termination, while the blue highlights H/I termination and brown *i*Pr/H and *i*Pr/*i*Pr termination.

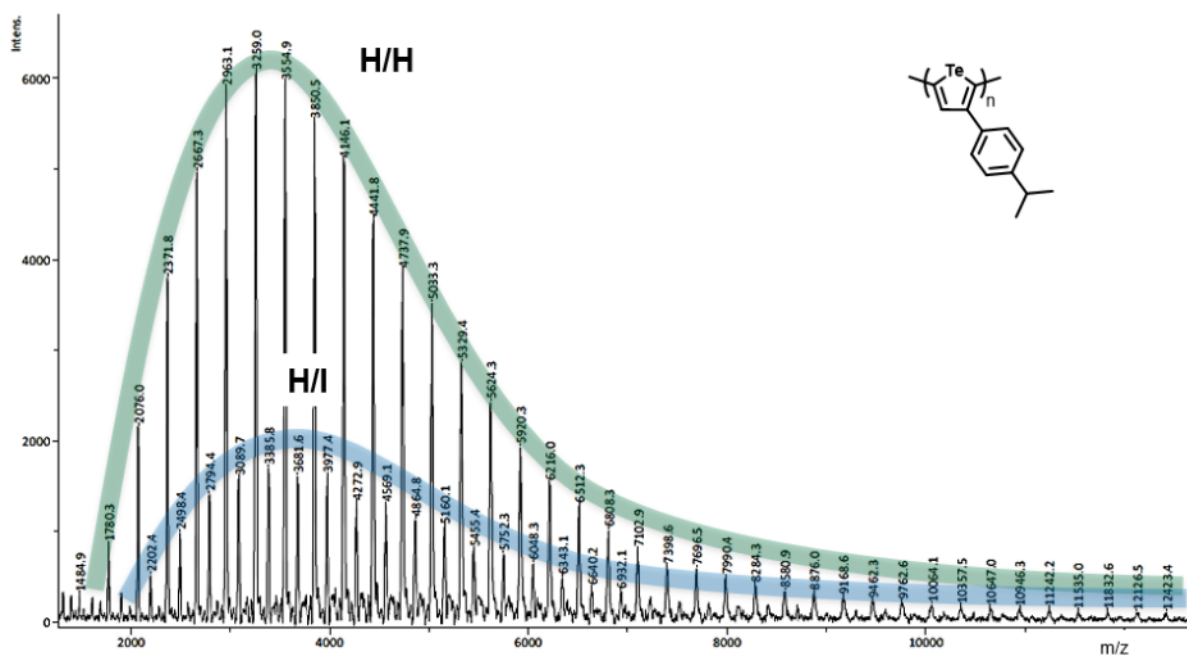


Fig. S37. MALDI-MS of PolyTe-cumenyl. Green curve highlights H/H termination, while the blue highlights H/I termination.

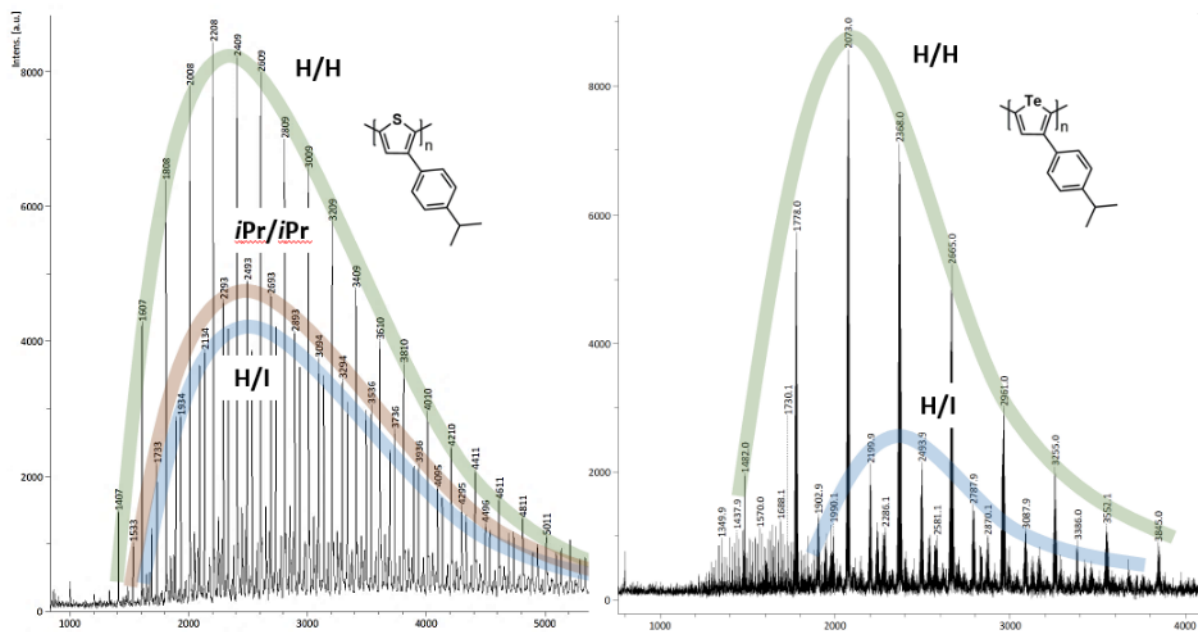


Fig. S38. MALDI-MS of **PolyS-cumenyl** and **PolyTe-cumenyl** prepared with $\text{Ni}(\text{dppf})\text{Cl}_2$ as a pre-catalyst. Green curve highlights H/H termination, while the blue highlights H/I termination and brown $i\text{Pr}/i\text{Pr}$. The polythiophene was prepared at 80 °C and the polytellurophene at 40 °C.

8. Gel Permeation Chromatography

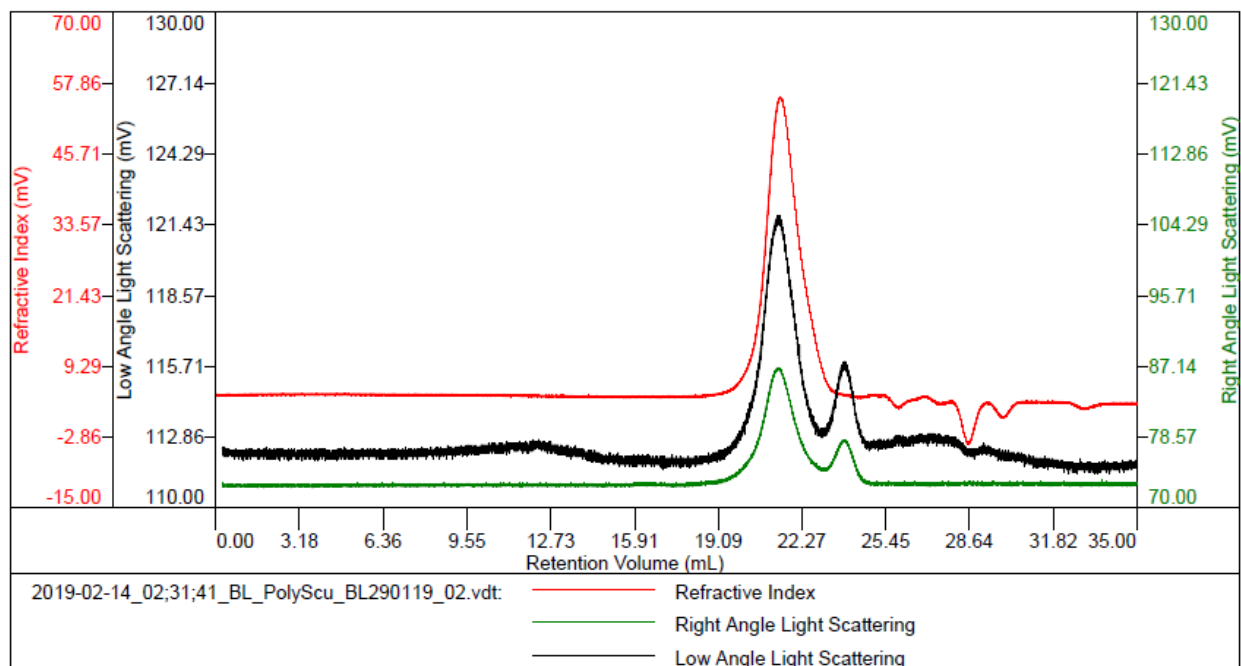


Fig. S39. GPC elution profile for **PolyS-cumenyl**. The negative peaks in the refractive index detector are artifacts of sample injection.

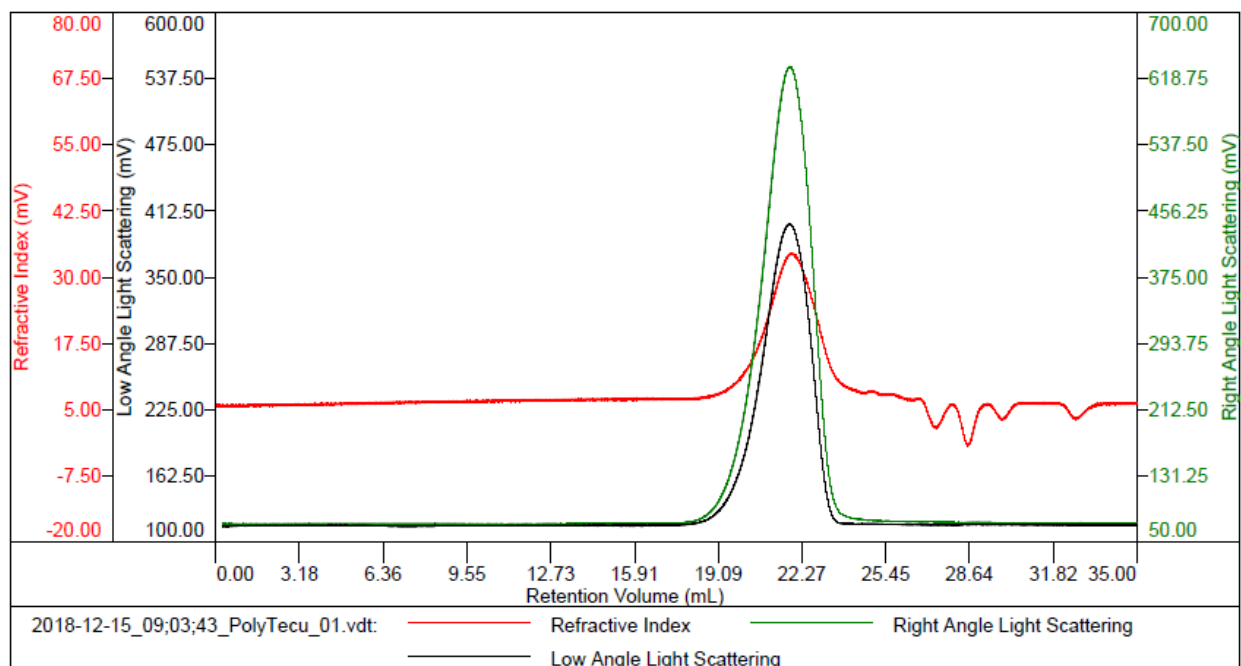


Fig. S40. GPC elution profile for **PolyTe-cumenyl**. The negative peaks in the refractive index detector are artifacts of sample injection.

9. TGA and DSC Data

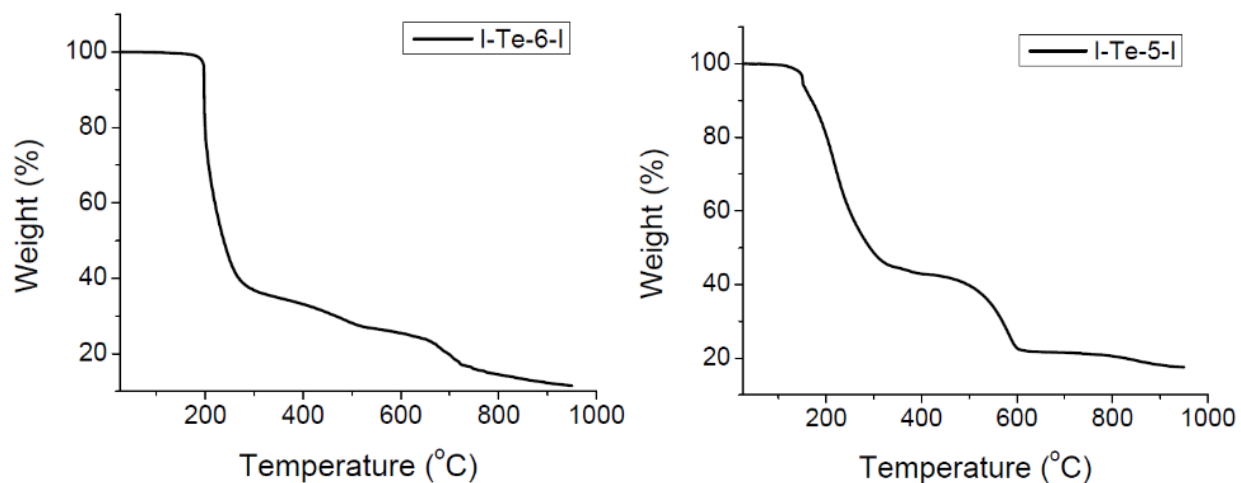


Fig. S41. TGA plots of I-Te-6-I (left) and I-Te-5-I (right) obtained at 10 °C/min under N₂.

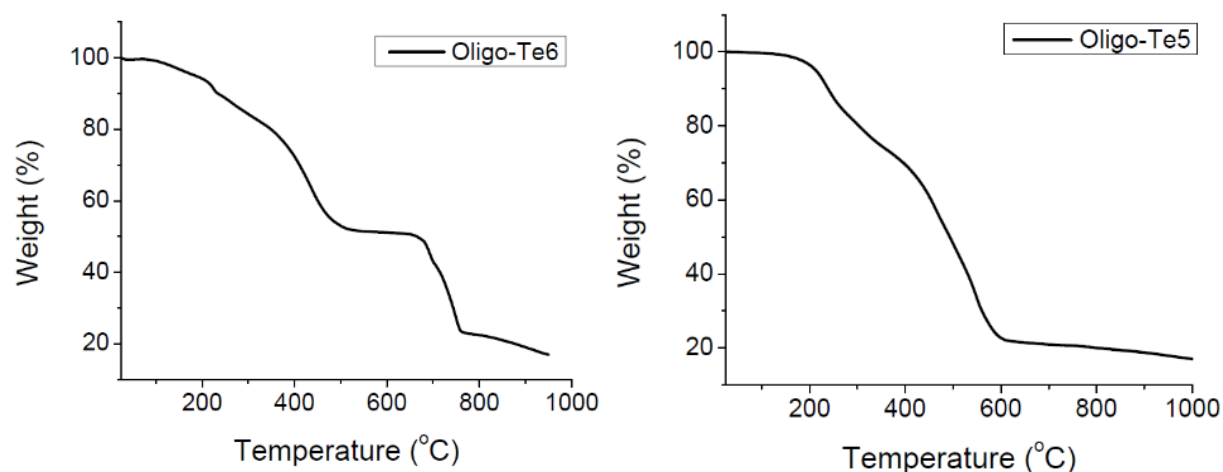


Fig. S42. TGA plots of Oligo-Te6 (left) and Oligo-Te5 (right) obtained at 10 °C/min under N₂.

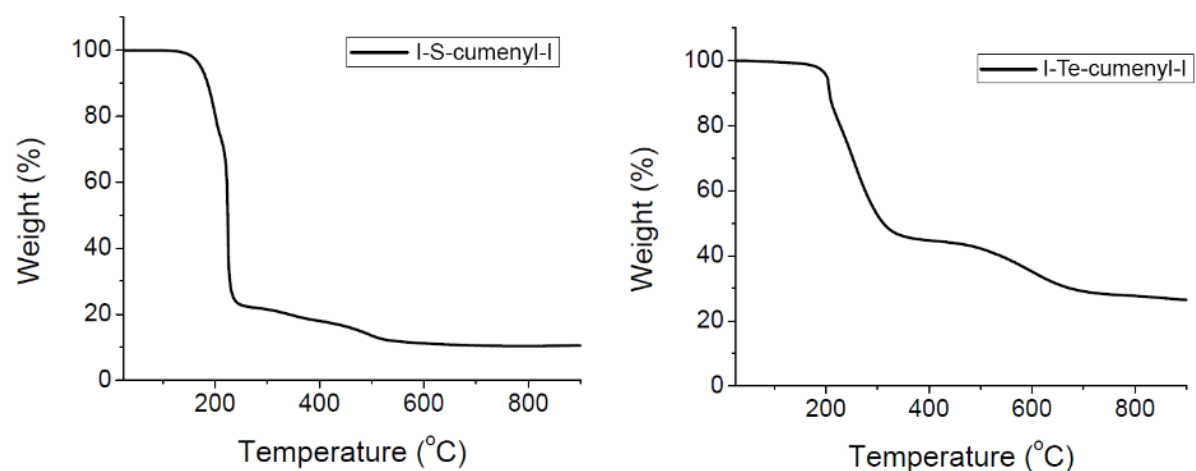


Figure S43. TGA plots of I-S-cumenyl-I (left) and I-Te-cumenyl-I (right) obtained at 10 °C/min under N₂.

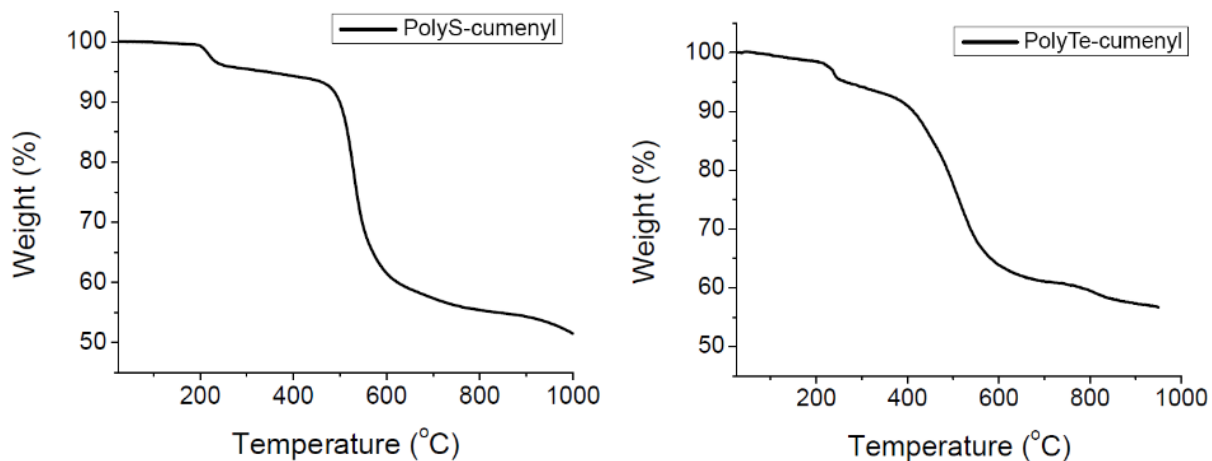


Fig. S44. TGA of **PolyS-cumenyl** (left) and **PolyTe-cumenyl** (right) obtained at 10 °C/min under N₂.

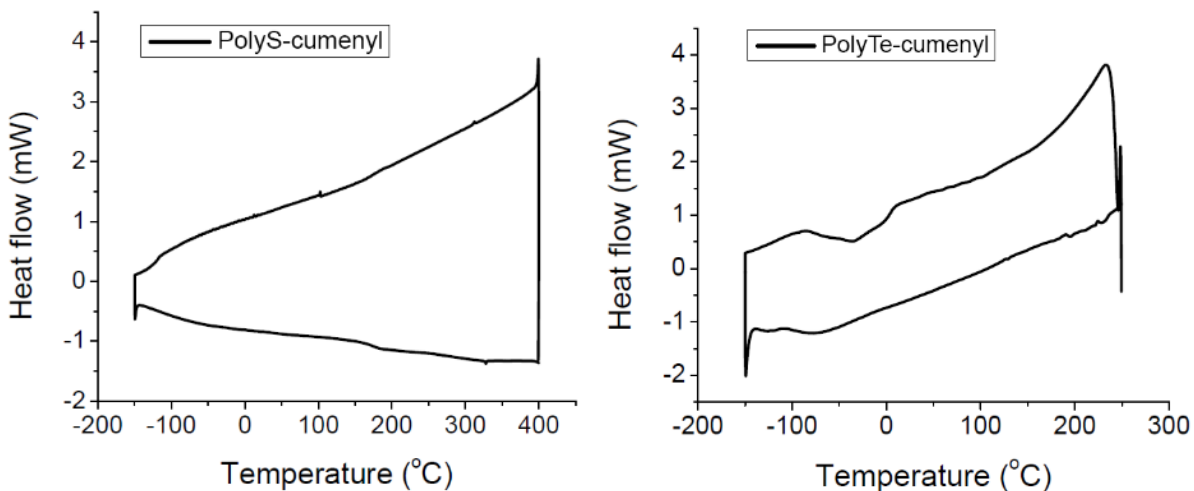


Fig. S45. DSC of **PolyS-cumenyl** (left) and **PolyTe-cumenyl** (right) obtained at 20 °C/min under N₂.

10. Cyclic Voltammetry

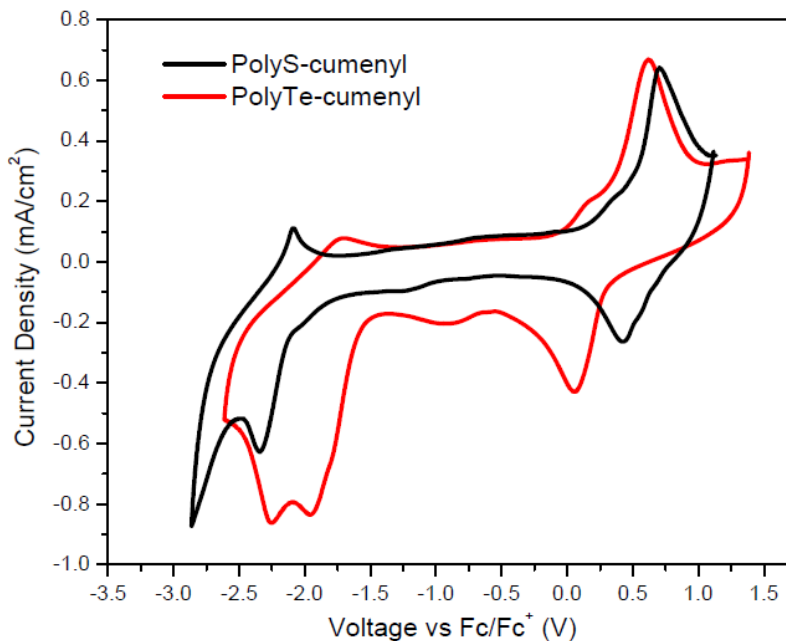


Fig. S46. Cyclic voltammogram of **PolyTe-cumenyl** and **PolyS-cumenyl** annealed films on ITO. Onset of oxidation at positive potentials: **PolyTe-cumenyl**: -0.05 V; **PolyS-cumenyl**: 0.15 V. Onset of reduction at negative potentials: **PolyTe-cumenyl**: -1.60 V; **PolyS-cumenyl**: -1.79 V. Scan rate 100 mV/s; electrolyte = 1.0 M ⁿBu₄N[PF₆] in CH₃CN.

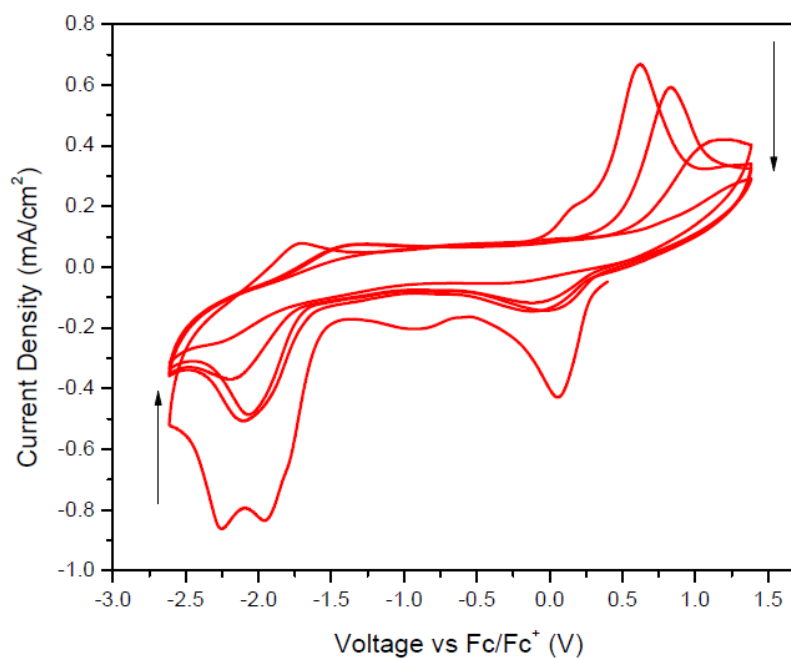


Fig. S47. Cyclic voltammogram of **PolyTe-cumenyl** over different cycles. Arrows show the direction of current intensity change. Scan rate 100 mV/s; electrolyte = 1.0 M ⁿBu₄N[PF₆] in CH₃CN.

11. Powder XRD

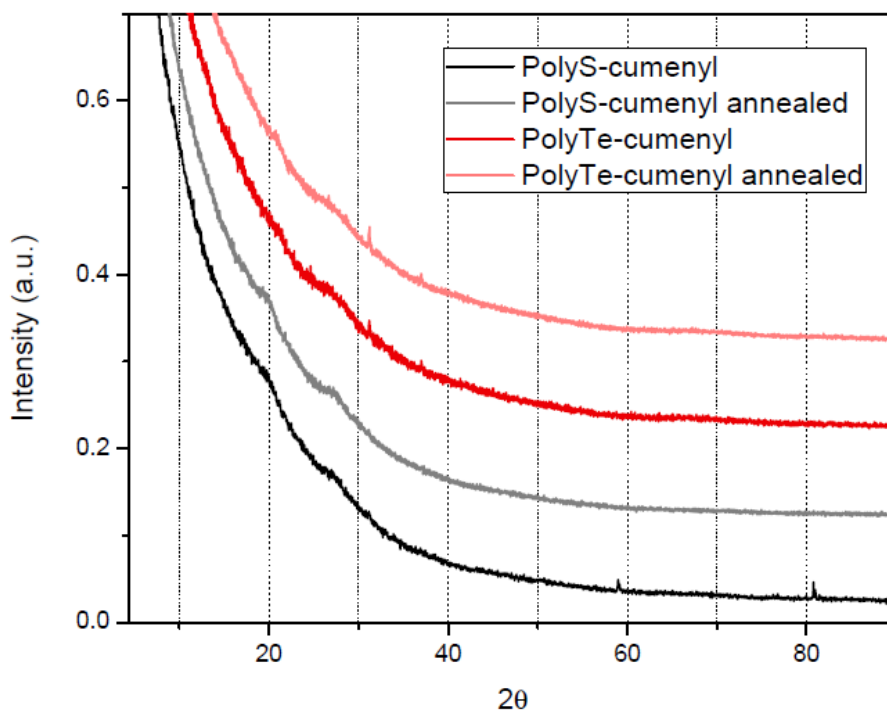


Fig. S48. Powder XRD of **PolyTe-cumenyl** and **PolyS-cumenyl** before and after solvent vapor annealing. The polymers were drop cast from 5 mg/mL CHCl_3 solutions and annealed by exposure to CHCl_3 vapor at 35 °C for one hour.

12. References

- 1 D. Barnes-Seeman, M. Jain, L. Bell, S. Ferreira, S. Cohen, X.-H. Chen, J. Amin, B. Snodgrass and P. Hatsis, *ACS Med. Chem. Lett.*, 2013, **4**, 514–516.
- 2 V. Gandon, D. Leca, T. Aechtner, K. P. C. Vollhardt, M. Malacria and C. Aubert, *Org. Lett.*, 2004, **6**, 3405–3407.
- 3 J. Lozada, Z. Liu and D. M. Perrin, *J. Org. Chem.*, 2014, **79**, 5365–5368.
- 4 J. L. Dutton, G. J. Farrar, M. J. Sgro, T. L. Battista and P. J. Ragona, *Chem. Eur. J.*, 2009, **15**, 10263–10271.
- 5 (a) G. He, W. Torres Delgado, D. J. Schatz, C. Merten, A. Mohammadpour, L. Mayr, M. J. Ferguson, R. McDonald, A. Brown, K. Shankar and E. Rivard, *Angew. Chem. Int. Ed.*, 2014, **53**, 4587–4591; (b) W. Torres Delgado, F. Shahin, M. J. Ferguson, R. McDonald, G. He and E. Rivard, *Organometallics*, 2016, **35**, 2140–2148.
- 6 T. R. Hoye, B. M. Eklov and M. Voloshin, *Org. Lett.*, 2004, **6**, 2567–2570.
- 7 A. Krasovskiy and P. Knochel, *Synthesis*, 2006, **5**, 890–891.
- 8 E. L. Tyson, M. S. Ament and T. P. Yoon, *J. Org. Chem.*, 2013, **78**, 2046–2050.
- 9 J. K. Yano, T. T. Denton, M. A. Cerny, X. Zhang, E. F. Johnson and J. R. Cashman, *J. Med. Chem.*, 2006, **49**, 6987–7001.
- 10 M. A. Truong, S. Fukuta, T. Koganezawa, Y. Shoji, M. Ueda and T. Higashihara, *J. Polym. Sci. Part A Polym. Chem.*, 2015, **53**, 875–887.

- 11 A. D. Becke, *J. Chem. Phys.*, 1993, **98**, 5648–5652.
- 12 C. Lee, W. Yang and R. G. Parr, *Phys. Rev. B*, 1988, **37**, 785–789.
- 13 A. Bennett, W. A. Shirley, M. A. Al-Laham, T. G. Tensfeldt, G. A. Petersson and J. Mantzaris, *J. Chem. Phys.*, 2002, **89**, 2193–2218.
- 14 G. A. Petersson and M. A. Al-Laham, *J. Chem. Phys.*, 1991, **94**, 6081–6090.
- 15 W. R. Wadt and P. J. Hay, *J. Chem. Phys.*, 1985, **82**, 284–298.
- 16 M. J. Frisch, G. W. Trucks, H. B. Schlegel, G. E. Scuseria, M. A. Robb, J. R. Cheeseman, G. Scalmani, V. Barone, G. A. Petersson, H. Nakatsuji, M. C. X. Li, A. Marenich, J. Bloino, B. G. Janesko, R. Gomperts, B. Mennucci, H. P. Hratchian, J. V. Ortiz, A. F. Izmaylov, J. L. Sonnenberg, D. Williams-Young, F. Ding, F. Lipparini, F. Egidi, J. Goings, B. Peng, A. Petrone, T. Henderson, D. Ranasinghe, V. G. Zakrzewski, J. Gao, N. Rega, G. Zheng, W. Liang, M. Hada, M. Ehara, K. Toyota, R. Fukuda, J. Hasegawa, M. Ishida, T. Nakajima, Y. Honda, O. Kitao, H. Nakai, T. Vreven, K. Throssell, J. A. J. Montgomery, J. E. Peralta, F. Ogliaro, M. Bearpark, J. J. Heyd, E. Brothers, K. N. Kudin, V. N. Staroverov, T. Keith, R. Kobayashi, J. Normand, K. Raghavachari, A. Rendell, J. C. Burant, S. S. Iyengar, J. Tomasi, M. Cossi, J. M. Millam, M. Klene, C. Adamo, R. Cammi, J. W. Ochterski, R. L. Martin, K. Morokuma, O. Farkas, J. B. Foresman and D. J. Fox, Gaussian 09, Revision A.02, *Gaussian, Inc., Wallingford CT*.
- 17 M. J. Frisch, G. W. Trucks, H. B. Schlegel, G. E. Scuseria, M. A. Robb, J. R. Cheeseman, G. Scalmani, V. Barone, G. A. Petersson, H. Nakatsuji, X. Li, M. Caricato, A. V. Marenich, J. Bloino, B. G. Janesko, R. Gomperts, B. Mennucci, H. P. Hratchian, J. V. Ortiz, A. F. Izmaylov, J. L. Sonnenberg, D. Williams-Young, F. Ding, F. Lipparini, F. Egidi, J. Goings, B. Peng, A. Petrone, T. Henderson, D. Ranasinghe, V. G. Zakrzewski, J. Gao, N. Rega, G. Zheng, W. Liang, M. Hada, M. Ehara, K. Toyota, R. Fukuda, J. Hasegawa, M. Ishida, T. Nakajima, Y. Honda, O. Kitao, H. Nakai, T. Vreven, K. Throssell, J. A. J. Montgomery, J. E. Peralta, F. Ogliaro, M. J. Bearpark, J. J. Heyd, E. N. Brothers, K. N. Kudin, V. N. Staroverov, T. A. Keith, R. Kobayashi, J. Normand, K. Raghavachari, A. P. Rendell, J. C. Burant, S. S. Iyengar, J. Tomasi, M. Cossi, J. M. Millam, M. Klene, C. Adamo, R. Cammi, J. W. Ochterski, R. L. Martin, K. Morokuma, O. Farkas, J. B. Foresman and D. J. Fox, Gaussian 16, Revision B.01, *Gaussian, Inc., Wallingford CT*.
- 18 M. D. Hanwell, D. E. Curtis, D. C. Lonie, T. Vandermeersch, E. Zurek and G. R. Hutchison, *J. Cheminf.*, 2012, **4**, Article 17.